Mostafa, M. H.; Mirmoosa, M. S.; Sidorenko, M. S.; Asadchy, V. S.; Tretyakov, S. A.

Temporal interfaces in complex electromagnetic materials: an overview [Invited]

Published in:
Optical Materials Express

DOI:
10.1364/ome.516179

Published: 01/05/2024

Document Version
Publisher's PDF, also known as Version of record

Please cite the original version:
Mostafa, M. H., Mirmoosa, M. S., Sidorenko, M. S., Asadchy, V. S., & Tretyakov, S. A. (2024). Temporal interfaces in complex electromagnetic materials: an overview [Invited]. *Optical Materials Express*, *14*(5), 1103-1127. https://doi.org/10.1364/ome.516179

Review | Vol. 14, No. 5 / 1 May 2024 / *Optical Materials Express* 1103

Optical Materials EXPRESS

Temporal interfaces in complex electromagnetic materials: an overview [Invited]

M. H. Mostafa,[1,*] M. S. Mirmoosa,[2] M. S. Sidorenko,[1] V. S. Asadchy,[1] and S. A. Tretyakov[1]

[1] *Department of Electronics and Nanoengineering, Aalto University, P.O. Box 15500, FI-00076 Aalto, Finland*

[2] *Department of Physics and Mathematics, University of Eastern Finland, P.O. Box 111, FI-80101 Joensuu, Finland*

[*] *mohamed.mostafa@aalto.fi*

Abstract: Time-varying metamaterials are currently at the forefront of research, offering immense possibilities for intriguing wave manipulations. Temporal modulations of metamaterials have paved the way for unconventional realizations of magnetless nonreciprocity, wave amplification, frequency conversion, pulse shaping, and much more. Here, we overview the fundamentals and recent advancements of temporal interfaces in isotropic, anisotropic, and bianisotropic materials and metamaterials. Delving into the fundamentals of temporal scattering in media of different material classes, we draw insightful comparisons with phenomena observed at spatial interfaces. We specifically emphasize the potential of time-switched anisotropic and bianisotropic metamaterials in unlocking extraordinary temporal scattering phenomena. Furthermore, an overview of possible platforms to realize time-varying bianisotropic metamaterials is provided. Concluding with a glimpse into the future, we make a research outlook for time-varying anisotropic and bianisotropic metamaterials, highlighting their potential in obtaining exotic photonic time crystals and other dynamic electromagnetic structures.

1. Introduction

Engineering scattering of electromagnetic waves stands as one of the central challenges in applied physics. Scattering can be controlled by tailoring the shapes of scatterers and adjusting the electromagnetic properties of materials from which the scatterers are made from. Even limiting our discussion to engineering linear effects, one may need to use conductors, dielectrics, magnetic materials, or the most general linear materials that are governed by linear relations between the four field vectors, bianisotropic materials.

In recent decades, efforts have been dedicated to engineer artificial materials with unusual electromagnetic properties, metamaterials, and their two-dimensional version, metasurfaces [1–4]. For some time, metamaterials have been limited to being engineered solely in space. However, it is evident that the means for controlling scattering by altering the scatterers in *space* (for instance, by changing its shape, size or spatial periodicity) are fundamentally limited. For example, the frequency of a wave scattered from time-invariant and linear object is always conserved. It became apparent that harnessing the *temporal* degree of freedom by tailoring some material properties in time paves the way to intriguing scattering phenomena. For example, breaking translational and reversal symmetry in time allows various frequency/energy density transformations and non-reciprocal phenomena, e.g. [5–13].

One of the most straightforward forms of having temporal inhomogeneities in material properties is rapid switching (faster than one cycle of the incident wave) of certain material parameters, giving rise to a temporal interface. Scattering of waves at temporal interfaces can be considered as an analogue to scattering of waves at spatial interfaces. When an electromagnetic wave approaches an interface that divides the whole space to half-spaces with distinct material

#516179 https://doi.org/10.1364/OME.516179
Journal © 2024 Received 19 Dec 2023; revised 22 Feb 2024; accepted 23 Feb 2024; published 2 Apr 2024

Optical Materials EXPRESS

properties, in the most general case a pair of waves – the transmitted and reflected ones – are created to satisfy the boundary conditions. The incident and scattered waves undergo transformation of wavelength and wavevector while preserving frequency and power density, due to the translational symmetry in time. In analogy, an abrupt change of material parameters in time creates time-refraction and time-reflection, at which the wavelength and wavevector are conserved, but the frequency and energy density may be transformed [14,15].

Even though temporal interfaces are intriguing in their own right, their significance is heightened as they serve as the building blocks for generally time-varying metamaterial [16–18] and photonic time crystals (PTCs). Specifically, photonic time crystals denote electromagnetic systems that undergo periodic variations in time while maintaining uniformity in space [19]. Such systems exhibit unusual properties such as having momentum band gaps [20–22] within which waves can be amplified exponentially [23]. By breaking down a dynamic electromagnetic system into multiple temporal interfaces, it is then sufficient to study the temporal interfaces to extrapolate the electromagnetic response of the dynamic electromagnetic system, as discussed in [24]. In this context, temporal interfaces serve as temporal meta-atoms of time-varying metamaterials [25].

We overview the current status of research on temporal interfaces in isotropic, anisotropic, and bianisotrpic metamaterials, along with potential platforms for their realization. It becomes evident that time-varying metamaterials can facilitate the realization of numerous exciting and practically useful field effects. Drawing an analogy with phenomena at spatial interfaces, where the use of more general metamaterials is necessary for complete control over scattering phenomena, we demonstrate that the full potential of time-varying metamaterials can be realized by exploring time-varying metamaterials that exhibit the most general properties, such as anisotropy and bianisotropy. Furthermore, we foresee the potential of time-varying anisotropic and bianisotropic metamaterials in exploiting exotic photonic time crystals.

2. Motivation: time-invariant bianisotropic slab

To emphasize the significance of contemplating time-varying general bianisotropic metamaterials and the necessity to understand wave phenomena in metamaterials with temporal inhomogeneities in all material parameters, we draw an analogy with well-understood *spatially* inhomogeneous metamaterials. Let us consider a simple illustrative example of electromagnetic scattering phenomena at a time invariant uniaxial bianisotropic spatial slab illuminated by a normally incident plane wave, as illustrated in Fig. 1. The example symmetry is uniaxial, that is, the only preferred direction is the normal to the slab boundaries, defined by the unit vector $\mathbf{n}$. We assume that the bianisotropic metamaterial inside the slab is homogenizable, so that we can model it with macroscopic material relations. Bianisotropic materials are the most general linear materials whose properties can be modeled by local linear relations between the four field vectors $\mathbf{E}$, $\mathbf{H}$, $\mathbf{D}$, and $\mathbf{B}$ at every point in space. In the frequency domain, these relations can be written as e.g. [26,27]

$$\begin{aligned}
\mathbf{D}(\omega) &= \overline{\overline{\varepsilon}}(\omega)\cdot\mathbf{E}(\omega) + \frac{1}{c}\left(\overline{\overline{\chi}}(\omega) - j\overline{\overline{\kappa}}(\omega)\right)\cdot\mathbf{H}(\omega), \\
\mathbf{B}(\omega) &= \overline{\overline{\mu}}(\omega)\cdot\mathbf{H}(\omega) + \frac{1}{c}\left(\overline{\overline{\chi}}(\omega) + j\overline{\overline{\kappa}}(\omega)\right)^T\cdot\mathbf{E}(\omega),
\end{aligned} \tag{1}$$

in which $\overline{\overline{\varepsilon}}(\omega)$ and $\overline{\overline{\mu}}(\omega)$ represent the permittivity and permeability dyadics, respectively. Magnetoelectric phenomena caused by weak spatial dispersion are measured by the coupling dyadic $\overline{\overline{\kappa}}(\omega)$ and those due to nonreciprocal effects by $\overline{\overline{\chi}}(\omega)$. T denotes the transpose operation, and c is the speed of light. In reciprocal media, $\overline{\overline{\chi}}(\omega) = 0$. Detailed discussions on bianisotropic media parameters and corresponding effects can be found e.g. in [27–30]. Due to the uniaxial symmetry, all the dyadic material parameters in the constitutive relations (1) are uniaxial dyadics, defined by their symmetric and antisymmetric parts as $\overline{\overline{a}} = a^{\rm co}\overline{\overline{I}}_t + a^{\rm cr}\mathbf{n}\times\overline{\overline{I}}_t$, where $\overline{\overline{I}}_t = \overline{\overline{I}} - \mathbf{nn}$

Optical Materials EXPRESS

is the two-dimensional unit dyadic in the transverse plane. Since for waves traveling along the axis **n** the longitudinal components of the fields are zero, we do not consider polarizations along vector **n**. In this case, the field-matter interactions are governed by eight scalar or pseudoscalar material parameters. In addition to the symmetric and antisymmetric parts of the permittivity and permeability, there are also the symmetric part of the reciprocal coupling coefficient κ (the chirality parameter) and the antisymmetric part Ω (the omega coupling parameter). The symmetric part of the nonreciprocal coupling dyadic $\overline{\overline{\chi}}$ is the Tellegen parameter χ, and the antisymmetric part corresponds to the artificial velocity V, see [27–29].

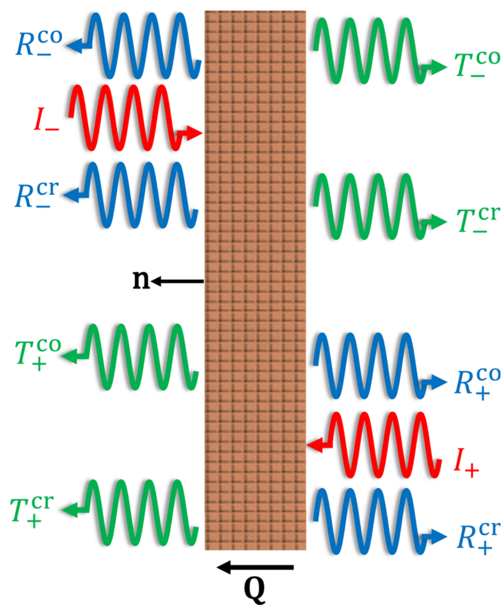

Fig. 1. A stationary uniaxial bianisotropic slab illuminated by normally incident plane waves from the right and left half-spaces, respectively. All eight possible transmitted and reflected waves are illustrated. The complex amplitudes denoted as I, T, and R correspond to incident, transmitted, and reflected waves. Superscripts co and cr stand for co-polarized and cross-polarized waves, respectively. Subscripts ± denote the directions of incidence ("+" for illumination from the right and "–" for illumination from the left). The external bias field **Q** can be, for instance, an external magnetic bias $\mathbf{B}_0$.

Let us list all possible scattering phenomena at the metamaterial slab. Suppose that there is a plane wave that illuminates the slab from the right (the incident wavevector is parallel to **n**). Obviously, this wave can be partially or fully transmitted in the same polarization or in the cross-polarized state. Likewise, reflections are possible in the co-polarized and in the cross-polarized state. This means that we need four parameters to characterize the scattering phenomena: co-and cross-polarized transmission coefficients $T_+^{\mathrm{co,cr}}$ and co-and cross-polarized reflection coefficients $R_+^{\mathrm{co,cr}}$. If we now illuminate the opposite side of the slab, so that the incident wavevector is antiparallel to the unit vector **n**, the response can be in general different, and we need four more parameters to describe the scattering phenomena: $T_-^{\mathrm{co,cr}}$ and $R_-^{\mathrm{co,cr}}$, being the co-and cross-polarized transmission and reflection coefficients respectively. Thus, in general we have eight parameters that fully define the response of the slab to plane-wave illuminations.

As we saw above, in the corresponding material relations (1) there are in general four material dyadics each of which is defined by symmetric and antisymmetric scalar material parameters. That is, we have exactly the same number of material parameters (eight) as the number of reflection and transmission coefficients that fully define the scattering phenomena at the metamaterial slab. This

Optical Materials EXPRESS

leads us to an important observation: In order to fully engineer the electromagnetic scattering at linear and time-invariant spatial inhomogeneities, the use of a bianisotropic material or metamaterial is imperative. Indeed, without bianisotropy there are only four material parameters (symmetric and anti-symmetric parts of the permittivity and permeability), so that we obviously do not have enough degrees of freedom to engineer all eight scattering coefficients. Only using all four additional material parameters of bianisotropic materials gives us all eight necessary degrees of freedom for controlling reflection and transmission in the most general way, limited only by the structure symmetry and fundamental restrictions on material parameter values.

In what concerns electromagnetic wave scattering at spatial inhomogeneities (slabs, metasurfaces, compact scatterers), the role of all material parameters of general bianisotropic media are well studied [30]. On the other hand, studies of inhomogeneities in time have been mostly limited to time-varying permittivity. There are some works on effects due to modulations of also permeability, but only a few initial studies that consider time-modulated bianisotropic media. Based on the above simple observations, it can be expected that time-varying bianisotropic metamaterials are needed to leverage the full richness of electromagnetic wave scattering at temporal inhomogeneities.

3. Temporal interfaces in isotropic, anisotropic, and bianisotropic metamaterials

Desired wave phenomena and transformations are often realized in interactions of electromagnetic waves with materials and metamaterials having spatial inhomogeneities of material properties, e.g. [1,31]. As elucidated earlier, the introduction of temporal inhomogeneities in material parameters expands the range of wave phenomena available for exploitation in wave-matter interactions [6–8,10,32,33]. In this section, we provide a concise overview of intriguing wave phenomena that become accessible when different material parameters undergo rapid temporal changes in isotropic, anisotropic, and bianisotropic media.

3.1. Temporal interfaces in isotropic media

3.1.1. Temporal scattering

Before we delve into complex time-varying metamaterials, we set the ground by reviewing scattering phenomena at temporal interfaces in simple isotropic materials. Let us consider a monochromatic plane wave propagating through a spatially homogeneous, unbounded, and non-dispersive linear material, in the absence of any sources, where permittivity $\varepsilon(t)$ and/or permeability $\mu(t)$ undergo a rapid change in time (the rise time is much shorter than the wave period [34]). The effects of such time discontinuity on a propagating wave depend on what physical quantities are being conserved and/or continuous while forcing the medium to change in time. Boundary conditions that dictate conservation of electric charge Q and magnetic flux Φ were introduced in 1958 by Morgenthaler [14]. These conditions imply continuity of electric displacement $\mathbf{D}(t = t_-) = \mathbf{D}(t = t_+)$ and magnetic flux density $\mathbf{B}(t = t_-) = \mathbf{B}(t = t_+)$, where t_- and t_+ signify the time instances immediately preceding and following the temporal interface, respectively. In various scenarios, particularly in cases involving dispersive media [35–42], plasma [43–46], or non-conserved electric charge Q [8], different boundary conditions apply leading to slightly different wave phenomena. By imposing the boundary conditions to general solutions involving two eigenwaves propagating in the opposite directions after the temporal interface (named time-refracted and time-reflected waves), one can find the time-refraction T and time-reflection R coefficients with respect to the electric field [14]

$$T = \frac{1}{2}\frac{v_2}{v_1}\left(\frac{Z_2}{Z_1} + 1\right), \tag{2}$$

Optical Materials EXPRESS

$$R = \frac{1}{2}\frac{v_2}{v_1}\left(\frac{Z_2}{Z_1} - 1\right), \tag{3}$$

where subscripts $1, 2$ indicate the material before and after the temporal interface, $Z_{1,2} = \sqrt{\frac{\mu_{1,2}}{\varepsilon_{1,2}}}$ are the wave impedances, and $v_{1,2} = \frac{1}{\sqrt{\varepsilon_{1,2}\mu_{1,2}}}$ are the phase velocities. These equations show that temporal scattering can be attributed to two distinct physical processes, temporal alteration of the wave impedance and temporal switching of the phase velocity [35,47] (see also a comment in [35]). Contrary to time-refraction, time-reflection diminishes to null when the wave impedance remains constant at the temporal interface [14,48], similar to reflections from impedance matched spatial interfaces. It is noteworthy that even when the phase velocity is conserved across the temporal interface, signifying frequency conservation (as will be demonstrated in the next subsection), temporal scattering phenomena persist. In cases involving reciprocal and isotropic media, the time-reflected wave has not only the same frequency, but also the identical polarization characteristics as the time-refracted wave. While theoretical investigations into time-reflection date back to 1960s [14,49,50], experimental confirmation of this phenomenon has been achieved recently. In 2016, experiments utilizing water waves confirmed its existence [51], and, more recently, in 2023, the phenomenon was observed in electromagnetic waves utilizing dynamic transmission lines operating at megahertz frequencies [52].

3.1.2. Frequency and wavelength transformations

Here we delve into transformations of the temporal and spatial properties of waves at spatial/temporal interfaces. To gain a comprehensive understanding, it is instructive to start with transformations at spatial interfaces. Consider a normally incident plane wave that encounters a flat spatial interface. As a result, a transmitted wave propagates in the second medium at a phase velocity denoted as v_2 while the incident wave propagates in the initial medium at a phase velocity v_1. Due to the translational symmetry of the structure in time, the frequency is conserved. Consequently, in the second medium the wavelength and the wavenumber undergo transformation contingent upon the ratio v_2/v_1 [26]. In contrast, at temporal interfaces the rapid change of the medium properties takes place uniformly in space (maintaining translational symmetry in space), leading to conservation of the spatial profile of the wave (e.g., conservation of the wavelength and wavenumber) [14]. Given the rapid temporal variation of the phase velocity $v(t)$ while preserving the wavelength, it follows that the frequency undergoes an abrupt change as [14]

$$\omega_2 = \pm\omega_1 \frac{v_2}{v_1}, \tag{4}$$

where ω_1 is the frequency before the temporal interface. Such frequency/wavelength transformations are illustrated graphically in Fig. 2. It is important to emphasize that when $\varepsilon(t)$ and $\mu(t)$ undergo a change that preserves the phase velocity, so that $v_1 = v_2$, the frequency becomes *conserved* through the interface, even though the wave impedance changes in time rapidly inducing time-refraction and time-reflection [50]. In this case, both spatial and temporal wave properties remain conserved, which is a distinctive phenomenon that has received relatively little attention. It is crucial to note that at temporal interfaces in isotropic metamaterials, the frequency transformation maintains symmetry with respect to both propagation directions and both circular polarizations. In Subsection 3.3, we explore the potential of inducing asymmetric frequency transformations in time-switched bianisotropic metamaterials.

3.1.3. Energy and momentum transformations

Noether's theorem [53] relates translational symmetries of a physical system with conservation laws. Continuous translational symmetry means invariance under any translation in space or time (without rotation). Consequently, in a system characterized by spatial (temporal) translational

Optical Materials EXPRESS

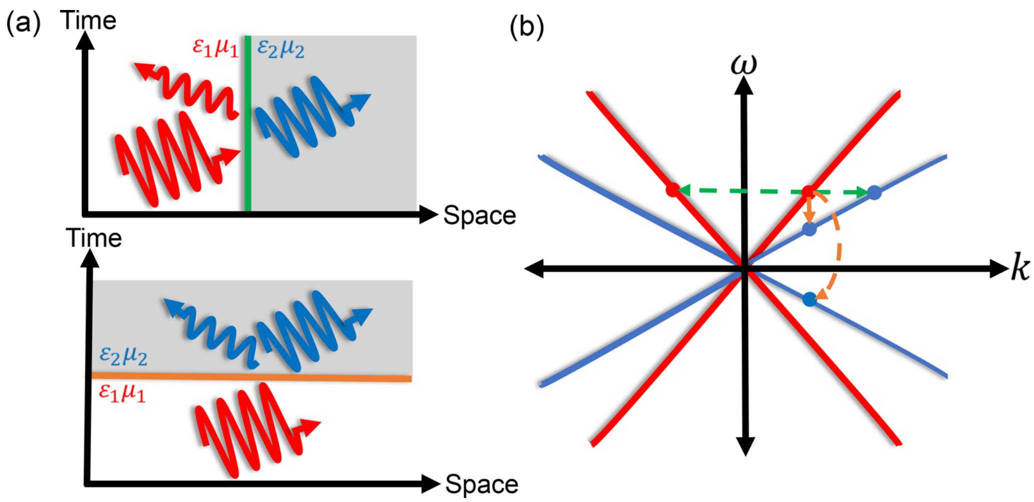

Fig. 2. (a) Scattering phenomena at spatial and temporal interfaces. (b) Illustration of transformations on the dispersion diagram, where the blue and red lines denote the dispersion of waves propagating in the two metamaterials with $\varepsilon_{1,2}$ and $\mu_{1,2}$. Angular frequency ω is conserved at the spatial interface, whereas the wavenumber k is conserved at the temporal interface.

symmetry, observations become independent of the observation point in space (time). According to the theorem, temporal translational symmetry results in the conservation of energy, whereas spatial translational symmetry leads to the conservation of linear momentum (Minkowski's momentum). Conservation of momentum at a temporal interface stems from the boundary conditions, as Minkowski's definition of linear momentum density is $\mathbf{P}_\mathrm{M} = \mathbf{D} \times \mathbf{B}$. Since the vectors $\mathbf{D}$ and $\mathbf{B}$ are continuous across temporal interfaces, Minkowski's linear momentum is conserved by definition. It is noteworthy that Abraham's linear momentum $\mathbf{P}_\mathrm{A} = \mathbf{E} \times \mathbf{H}$ is not generally conserved at a temporal interface. For further details regarding conservation of linear momentum in time-varying metamaterials the reader is referred to a recent tutorial [54]. On the other hand, time modulations of media obviously break translational symmetry in time. Thus, Noether's theorem predicts that the energy is not conserved at a temporal interface, which has been theoretically shown in [14].

Let us go back to our temporal interface (involving nondispersive media) and consider the electric volume energy density $w^\mathrm{e} = \frac{1}{2}\varepsilon\mathbf{E}\cdot\mathbf{E}$ and magnetic volume energy density $w^\mathrm{m} = \frac{1}{2}\mu\mathbf{H}\cdot\mathbf{H}$. For a plane wave, the total volume energy density before the temporal interface is $u_1 = w_1^\mathrm{e} + w_1^\mathrm{m} = \varepsilon_1\mathbf{E}_1 \cdot \mathbf{E}_1$. Assuming that there is a temporal interface at $t = 0$, the ratio of the total volume energy density after the interface $u_2 = w_2^\mathrm{e} + w_2^\mathrm{m}$ and u_1 can be found from (2) and (3): $\frac{u_2|_{t=0}}{u_1|_{t=0}} = \frac{1}{2}(\frac{\varepsilon_1}{\varepsilon_2} + \frac{\mu_1}{\mu_2})$ [14]. This result can be reformulated in terms of the phase velocities and wave impedances as [47]

$$\frac{u_2|_{t=0}}{u_1|_{t=0}} = \frac{1}{2}\frac{v_2}{v_1}\left(\frac{Z_1}{Z_2} + \frac{Z_2}{Z_1}\right). \tag{5}$$

We see that the amount of gain or loss in energy density at a temporal interface is determined by the changes in the phase velocity and the wave impedance. It is noteworthy that the energy transformation directly stems from the imposed boundary conditions at the temporal interface, as they determine the scattering coefficients in (2) and (3), which, in turn, are employed to derive (5). While the common assertion often links the alteration in energy to frequency conversion, it is apparent from (5) that even if the phase velocity remains constant, preserving the frequency, there is still a jump in energy density attributable to the abrupt change in the wave impedance.

In addition, when the phase velocity is preserved at a temporal interface, the energy density is always greater after the temporal interface, since $Z_1^2 + Z_2^2 > 2Z_1Z_2$. These observations have practical significance, showing potential for efficient amplification through time modulation while avoiding frequency conversion and reversed energy flow. Furthermore, the energy becomes conserved at the temporal interface when $\frac{\varepsilon_1}{\varepsilon_2} + \frac{\mu_1}{\mu_2} = 2$, even though the frequency is transformed and time-refraction and time-reflection persist. Similar to frequency transformations at temporal interfaces in isotropic materials, energy transformations are the same for both propagation directions and both circular polarizations. In Subsection 3.3, we explore the potential of inducing asymmetric energy transformations in time-switched bianisotropic media.

3.2. Temporal interfaces in anisotropic media

The next step towards exploring more complex time-varying materials is to comprehend phenomena involving anisotropic features. In particular, let us discuss the case when materials suddenly change from an isotropic state to an anisotropic one (or vice versa), creating a temporal discontinuity of such spatial symmetries. The anisotropy can show itself in the electric response (represented by the permittivity tensor) and/or in the magnetic response (measured by the permeability tensor). Considering only the electric response, we write the effective permittivity tensor of an anisotropic material after the discontinuity as

$$\overline{\overline{\varepsilon}} = \varepsilon_0 \begin{pmatrix} \varepsilon_{xx} & \varepsilon_{xy} & 0 \\ \varepsilon_{yx} & \varepsilon_{yy} & 0 \\ 0 & 0 & \varepsilon_{zz} \end{pmatrix}, \tag{6}$$

in which ε_0 is the free-space permittivity and ε_{ij} denotes the elements of the relative permittivity tensor. In the following, we briefly show the significant difference compared to the isotropic case that we explained in the previous subsection. For simplicity, we consider fast transitions from free space to a nondispersive and uniaxially anisotropic dielectric material with $\varepsilon_{xy} = \varepsilon_{yx} = 0$ and $\varepsilon_{xx} = \varepsilon_{yy} \neq \varepsilon_{zz} > 0$. Eigenwaves of two polarizations exist in such media. Here, we concentrate on the polarization that possesses an exotic isofrequency surface, which is the transverse magnetic one. The waves with this polarization obey the following dispersion relation: $k_z^2/\varepsilon_{xx} + k_x^2/\varepsilon_{zz} = \omega^2/c^2$, in which k_z and k_x are the wavevector components in the z and x directions, respectively. This dispersion relation defines an elliptic isofrequency contour in the **k**-space. However, the isofrequency contour for free space is a circle that corresponds to the dispersion relation of $k_x^2 + k_z^2 = \omega^2/c^2$. We already know that at the temporal interface, the wavevector is conserved. Therefore, due to the difference between the isofrequency contours associated with the media before and after the temporal jump, it is easy to see that the converted angular frequency depends on the wavevector components of the wave before the temporal interface. Indeed, after an algebraic manipulation, we derive that

$$\omega_2^2 = \frac{1}{\varepsilon_{xx}}\omega_1^2 + k_x^2 c^2 \Big(\frac{1}{\varepsilon_{zz}} - \frac{1}{\varepsilon_{xx}}\Big), \tag{7}$$

where $\omega_{1,2}$ are the angular frequencies before and after the temporal interface. Equation (7) explicitly confirms that the new angular frequency is a function of the transverse component of the wavevector k_x, a salient property that is absent in the case of the isotropic scenario (see Eq. (4)). It is worth noting that since the Poynting vector is normal to the isofrequency contour, such temporal discontinuity may also drastically affect the direction of the flow of power.

Several research groups have contemplated temporal interfaces in anisotropic media. Probably, the initial efforts were done about two decades ago in studies of the rapid creation of plasma media in the presence of a static magnetic field [55]. In that setting, it is assumed that a uniform

Optical Materials EXPRESS

plane wave is traveling in free space, filling the whole space, in the presence of an external static space-uniform magnetic field. At $t = 0$, suddenly, the whole space is ionized, and, consequently, this transforms the medium from free space to a magnetoplasma medium. In consequence, it is proved that different polarizations (right-handed and left-handed circular polarizations) will propagate after the temporal discontinuity with different angular frequencies. Therefore, as a result of such temporal discontinuity, controlling polarization states of electromagnetic waves is achieved. Recently, following this research direction, in Refs. [56] and [57], it was shown that temporal interfaces in anisotropic media also provide a possibility of spin-dependent polarization conversion and analog computing. Besides polarization manipulation, other interesting phenomena have been uncovered, such as redirecting the energy of propagating waves which is called temporal aiming [58], temporal equivalent of the Brewster angle [59], and implementation of an inverse prism [60] where the electromagnetic waves propagating in different directions but at the same frequency are transformed into waves that propagate at different frequencies while keeping the same directions. Some of the interesting phenomena explained above are shown in Fig. 3.

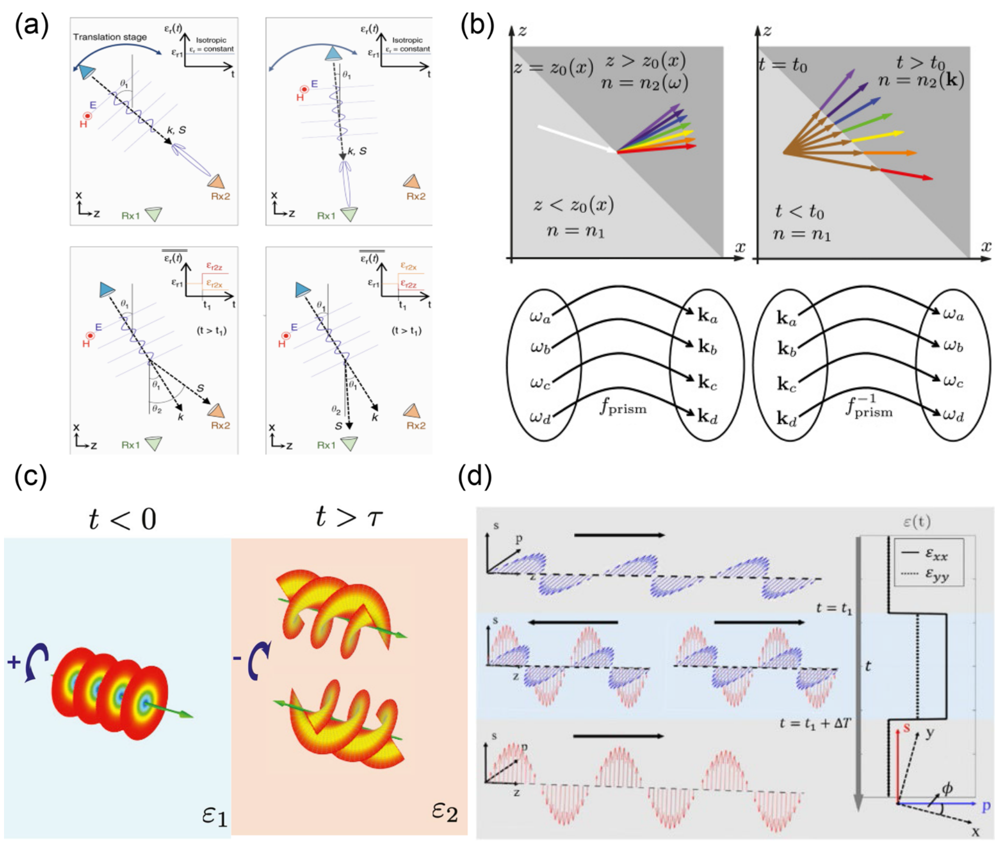

Fig. 3. Different phenomena uncovered by the creation of temporal interfaces in anisotropic media. (a) Temporal aiming (adapted from [58]). (b) Inverse prism (adapted with permission from [60]). (c) Spin-controlled photonics via temporal anisotropy (adapted with permission of De Gruyter, from [57]; permission conveyed through Copyright Clearance Center, Inc.) (d) Polarization conversion (adapted with permission from [56]).

Optical Materials EXPRESS

3.3. Temporal interfaces in bianisotropic media

In order to achieve full control over electromagnetic waves, it is essential to enable direction-dependent and polarization-dependent phenomena at temporal interfaces. However, the insensitivity of temporal scattering in isotropic media to the direction of propagation and field polarization is evident from Eqs. (2), (3), (4), and (5). As conceived from the example in Section 2, introducing anisotropy is not sufficient to obtain general control over scattered fields. In order to break the symmetry of temporal scattering of waves having different propagation directions and polarizations, it becomes imperative to utilise bianisotropic media whose wave impedance and phase velocity depend on the propagation direction and polarization, as these are the two parameters that govern the temporal scattering phenomena (see Section 3.1.1). Next, we define the material relations and parameters of general bianisotropic media in time domain. Subsequently, we furnish an overview of intriguing scattering phenomena attainable at bianisotropic temporal interfaces.

3.3.1. Bianisotropic material relations in time domain

The time-domain counterparts of Eqs. (1), even for time-invariant media, contain convolution integrals due to nonlocality in time dubbed as temporal or frequency dispersion [61]. Only if we neglect such frequency dispersion, the relations become simple enough and allow analytical solutions for identifying and classifying possible field effects. For nonreciprocal magnetoelectric coupling material parameters (the Tellegen and the artificial velocity parameters), we can assume that their frequency dispersion is negligible and use the material relations in the Tellegen form also in the time domain (see Eqs. (1)). However, this is not possible for the reciprocal coupling coefficients, because the very nature of these effects is spatial dispersion in the medium as discussed in [27], Sections 2.9 and 4.2. Therefore, in the frequency domain, these parameters must depend on the frequency. In particular, in the limit of zero frequency, they always tend to zero as linear functions of the frequency.

In order to be able to study time-varying bianisotropic media analytically, it is possible to restrict the analysis to the cases of weakly dispersive media and adopt the Condon model [62,63] to describe the corresponding coupling effects in the time domain. In this approximation, the general bianisotropic time-domain material relations are written in the form

$$\begin{aligned} \mathbf{D}(t) &= \overline{\overline{\varepsilon}}\cdot\mathbf{E}(t) + \frac{\chi}{c}\mathbf{H}(t) - \frac{\kappa}{c}\frac{\partial \mathbf{H}(t)}{\partial t} + \frac{V}{c}\mathbf{n}\times\mathbf{H}(t) + \frac{\Omega}{c}\mathbf{n}\times\frac{\partial \mathbf{H}(t)}{\partial t}, \\ \mathbf{B}(t) &= \overline{\overline{\mu}}\cdot\mathbf{H}(t) + \frac{\chi}{c}\mathbf{E}(t) + \frac{\kappa}{c}\frac{\partial \mathbf{E}(t)}{\partial t} - \frac{V}{c}\mathbf{n}\times\mathbf{E}(t) + \frac{\Omega}{c}\mathbf{n}\times\frac{\partial \mathbf{E}(t)}{\partial t}. \end{aligned} \tag{8}$$

For simplicity, we consider only uniaxial structure (the axis is along the unit vector $\mathbf{n}$), in which case the Tellegen and chirality parameters are scalar quantities. Since in this model of magnetoelectric coupling we retain only the first-order spatial dispersion effects (proportional to ω), we should neglect artificial magnetism, as this is a second-order effect [27]. It is worth noting that since these expressions are applicable at any point in space, for brevity, we do not include the position vector as an independent variable for the fields ($\mathbf{E}$, $\mathbf{H}$) and the flux densities ($\mathbf{D}$, $\mathbf{B}$). In Eq. (8), we observe that while the nonreciprocal terms χ and V are dimensionless (similarly to their frequency-domain counterparts described above), the dimension of the reciprocal terms κ and Ω in Eq. (8) is seconds. In this model, the assumption is that the field oscillations are at frequencies that are well below the resonances of material response, where the Condon model with constant coupling coefficients remains valid. This is a physically valid model that properly accounts for the inevitable frequency dispersion of chirality and omega coupling. In particular, for temporally constant fields ($\partial\mathbf{E}/\partial t = \partial\mathbf{H}/\partial t = 0$), the reciprocal coupling vanishes, which corresponds to the fact that there is neither chiral nor omega coupling in statics. In conclusion, the investigation of temporal interfaces necessitates the use of time-domain material relations,

Optical Materials EXPRESS

prompting the application of the Condon model in the case of temporal interfaces in bianisotropic media. This model is utilized to retrieve some of the results shown in the next subsection.

As we see from (2) and (3), the reflection and transmission coefficients are determined by the values of phase velocity and wave impedance before and after a time jump. For this reason, we list the effective phase velocity for each class of bianisotropic media (expressed for time-harmonic fields in the frequency domain) [64]:

$$\begin{aligned}
\text{chiral:} v_\kappa^{\circlearrowright} &= \left(\sqrt{\varepsilon\mu} - \frac{\omega\kappa}{c}\right)^{-1}, \quad v_\kappa^{\circlearrowleft} = \left(\sqrt{\varepsilon\mu} + \frac{\omega\kappa}{c}\right)^{-1}, \\
\text{Tellegen:} v_\chi &= \left(\sqrt{\varepsilon\mu - \frac{\chi^2}{c^2}}\right)^{-1}, \\
\text{omega:} v_\Omega &= \left(\sqrt{\varepsilon\mu - \frac{\omega^2\Omega^2}{c^2}}\right)^{-1}, \\
\text{artificial velocity:} v_V^{\rightarrow} &= \left(\sqrt{\varepsilon\mu} - \frac{V}{c}\right)^{-1}, \quad v_V^{\leftarrow} = \left(\sqrt{\varepsilon\mu} + \frac{V}{c}\right)^{-1},
\end{aligned} \tag{9}$$

and the corresponding wave impedances:

$$\begin{aligned}
\text{chiral:} Z_\kappa &= \sqrt{\frac{\mu}{\varepsilon}}, \\
\text{Tellegen:} Z_\chi^{\circlearrowright} &= \sqrt{\frac{\mu}{\varepsilon}}\left(\sqrt{1 - \frac{\chi^2}{n^2}} - j\frac{\chi}{n}\right), \quad Z_\chi^{\circlearrowleft} = \sqrt{\frac{\mu}{\varepsilon}}\left(\sqrt{1 - \frac{\chi^2}{n^2}} + j\frac{\chi}{n}\right), \\
\text{omega:} Z_\Omega^{\rightarrow} &= \sqrt{\frac{\mu}{\varepsilon}}\left(\sqrt{1 - \frac{\omega^2\Omega^2}{n^2}} + j\frac{\omega\Omega}{n}\right), \quad Z_\Omega^{\leftarrow} = \sqrt{\frac{\mu}{\varepsilon}}\left(\sqrt{1 - \frac{\omega^2\Omega^2}{n}} - j\frac{\omega\Omega}{n}\right), \\
\text{artificial velocity:} Z_V &= \sqrt{\frac{\mu}{\varepsilon}}.
\end{aligned} \tag{10}$$

Here, n, $\circlearrowright$, $\circlearrowleft$, $\rightarrow$, and $\leftarrow$ indicate refractive index, right-handed circular polarization, left-handed circular polarization, positive propagation direction, and negative propagation direction. We see that the key parameters that govern the scattering phenomena at temporal interfaces in bianisotropic media depend on the propagation direction and polarization, which shows possibilities for rather general control of temporal scattering. Some examples are discussed next.

3.3.2. Phenomena at temporal interfaces in bianisotropic media

Consider a harmonic plane wave propagating in a spatially uniform bianisotropic medium, where the bianisotropy vanishes rapidly at a specific moment in time (homogeneously in space) such that the bianisotropic coupling coefficient becomes zero. By applying the Condon model, one can prove that the expressions for the temporal scattering coefficients, the energy balance coefficient and the frequency transformation at temporal interfaces where bianisotropy is switched off are the same as the ones shown in (2), (3), (5), and (4) upon substituting the respective bianisotropic wave impedances and phase velocities into these expressions [64]. It is important to note that at a temporal interface where the magnetoelectric coupling is being switched on, the expressions in (2), (3), (5), and (4) do not generally apply, as frequency dispersion leads to excitation of waves at multiple frequencies, which is fundamentally different from what is studied above. Next, we review some of the recent results that were presented in [64]. At a chiral temporal interface, the scattered fields' amplitude, frequency, and energy exhibit a dependence on the handedness of the circular polarization. While at an artificial velocity temporal interface, the scattered fields' amplitude, frequency, and energy exhibit a dependence on the wave propagation direction. On the other hand, at a Tellegen temporal interface, only the *phase* of the scattered fields depends on the handedness of the circular polarization. Still, this asymmetric phase shift induces asymmetric polarization rotations in time-reflected and time-refracted waves. Finally, at an omega temporal interface, only the *phase* of the scattered fields depends on the propagation direction. Such asymmetric temporal scattering [64] is unattainable at temporal interfaces in isotropic or anisotropic media. Frequency and energy transformations at temporal interfaces in different bianisotropic media are summarised in Table 1 and illustrated in Fig. 4.

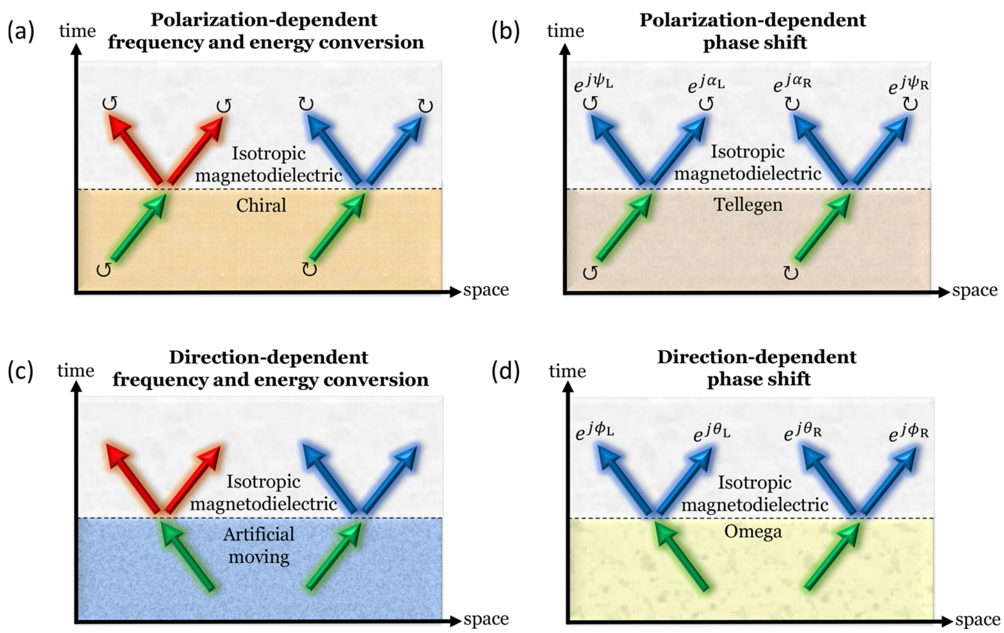

Fig. 4. A schematic illustration of different scattering phenomena at single temporal interfaces between bianisotropic media of different classes and a magnetodielectric [64]. Different colors indicate different frequencies and energy densities, rotating arrows indicate handedness of circular polarization, and the complex exponentials indicate the phase shifts taking place at temporal interfaces. Figures adapted from [64].

Table 1. Classification of different scattering phenomena (in transmission and reflection) at single spatial and temporal interfaces between different classes of bianisotropic and magnetodielectric media [64]. The scattering phenomena either depend on the circular polarization of the propagating wave or its direction of propagation.

Class	Phenomena dependance	Phenomena at spatial interface	Phenomena at temporal interface
Chiral	Polarization-dependent	Wavelength and momentum conversion	Frequency and energy conversion
Moving	Direction-dependent	Wavelength and momentum conversion	Frequency and energy conversion
Tellegen	Polarization-dependent	Phase shift	Phase shift
Omega	Direction-dependent	Phase shift	Phase shift

This potential of general control over the scattered fields opens avenues for intriguing wave phenomena. Considering chiral media, it was shown that due to polarization-dependent temporal scattering at chiral temporal interfaces, a linearly polarized wave splits into its two circularly polarized components, each distinguished by a unique frequency, as shown in Fig. 5(a) [65]. In addition, the authors demonstrated that within this phenomenon, the wave of one polarization experiences amplification, while the wave of the other polarization undergoes attenuation.

Optical Materials EXPRESS

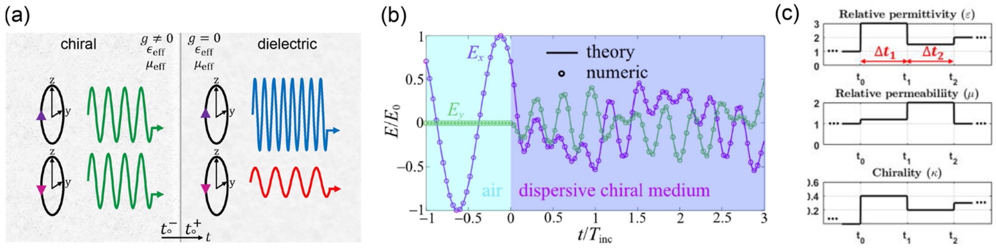

Fig. 5. (a) Polarization dependent frequency and energy transformations at a chiral temporal interface leading to splitting of linearly polarized light (adapted with permission of De Gruyter, from [65]; permission conveyed through Copyright Clearance Center, Inc.) (b) Multi-frequency temporal scattering at a dispersive chiral temporal interface exhibiting optical activity (adapted with permission from [66]). (c) Investigation of an arbitrary temporally varying chiral medium (reprinted from [67], with the permission of AIP Publishing).

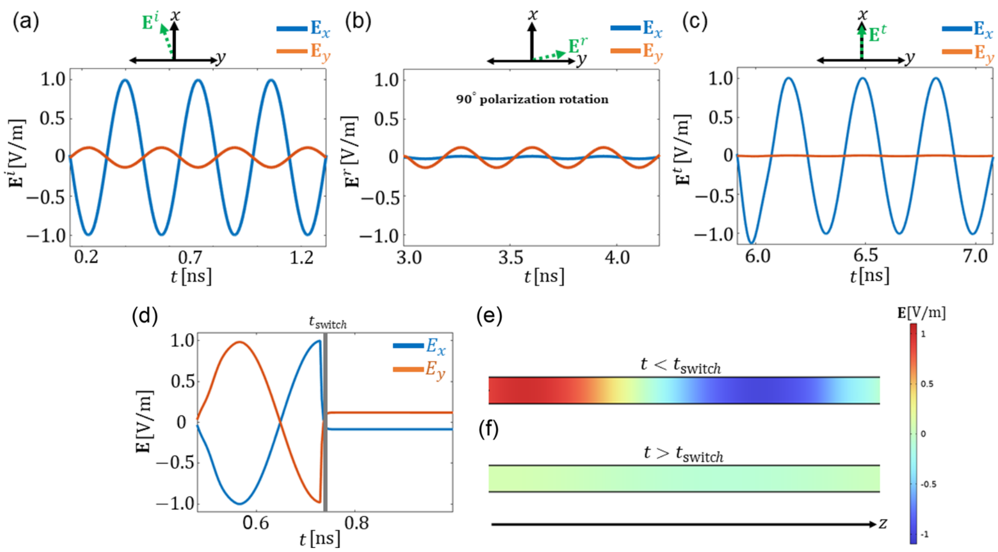

Fig. 6. (a)-(c) Simulation of a 90° polarization rotation in reflection at a time interface between Tellegen and magnetodielectric media [64], where (a)–incident electric field $\mathbf{E}^i$, (b)–reflected electric field $\mathbf{E}^r$ after the time interface, and (c)–transmitted electric field $\mathbf{E}^t$ after the time interface. The effective material parameters for the Tellegen medium are $\chi = 0.5$, $\varepsilon = 4\epsilon_0$, and $\mu = \mu_0$ (ε_0 and μ_0 are the free-space permittivity and permeability, respectively). The magnetodielectric medium has $\chi = 0$, $\varepsilon_\mathrm{m} = 3.75\varepsilon_0$, and $\mu_\mathrm{m} = \mu_0$. The incident electric field possesses x and y components, while the corresponding plane wave is propagating in the z direction. We observe a 90° polarization rotation in reflection. Furthermore, the transmitted wave also undergoes a slight polarization rotation. (d)-(f) Simulation of field evaporation at a time interface between Tellegen and magnetodielectric media [64], where (d)–temporal evolution of the electric field before and after the time interface, (e)–spatial distribution of the electric field before the time interface, and (f)–spatial distribution of the electric field after the time interface. The effective material parameters for the Tellegen medium are $\chi = 1.414$, $\varepsilon = 2\varepsilon_0$, and $\mu = \mu_0$. The magnetodielectric medium has $\chi = 0$, $\varepsilon_\mathrm{m} = 2\varepsilon_0$, and $\mu_\mathrm{m} = \mu_0$. We observe that, after the time interface, the frequency and amplitude become negligibly small. Figures adapted from [64].

Furthermore, a Lorentzian dispersive chiral temporal interface was contemplated in [66], where multi-frequency temporal scattering takes place, including excitation of backward propagating waves, as illustrated in Fig. 5(b). Lastly, a chiral medium with arbitrary temporal variation is investigated in [67] (Fig. 5(c)). On the other hand, considering Tellegen media, it was shown that time-reflected and time-refracted waves undergo asymmetric polarization rotations at time interfaces between Tellegen and magnetodielectric media [64]. The authors demonstrated a complete 90-degree rotation in the time-reflected wave, while the time-refracted wave undergoes slight polarization rotation, as shown Fig. 6(a)-(c). Moreover, it has also been shown that when a Tellegen medium has zero effective refractive index, and then it is switched to a magnetodielectric medium, the propagating fields experience evaporation [64], resulting in negligible amplitude and nearly zero frequency, as shown in Fig. 6(d)-(f). An outlook for time-varying bianisotrpic media is provided in Section 5.

4. Typical structures of bianisotropic materials and discussion of possible implementations of such time-varying systems

Practical realization of time-varying media poses numerous challenges. However, there have been multiple successful realizations recently, revealing the richness of possible approaches for time modulation of material properties. To name a few, time-reflection (time reversal) of water waves has been demonstrated experimentally in [51]. More recently, time-reflection of electromagnetic waves has been also demonstrated by utilizing time-modulated transmission lines [52,68]. In addition, momentum band gaps have been observed in periodically time-varying transmission lines [69], and periodically time-varying metasurfaces [23]. Finally, recent efforts succeeded to observe time-refraction at optical frequencies [70,71]. Most of the experimental realizations leverage phenomena in isotropic media. On the other hand, there are several scenarios that one may ponder to realize time-varying anisotropic media modeled by Eq. (6). For instance, it is possible to apply a magnetic bias field at a specific moment in time to a plasma volume [72] or time modulate magnetic bias of a ferrite sample. Another possibility is to use electronic devices to control currents in wire metamaterials [73].

Next, we discuss in some detail the possibilities to obtain time-varying bianisotropic media. First, it is important to examine realizations of usual, non-varying bianisotropic media, to be able to select most suitable means to modulate bianisotropy in time. While numerous natural materials exhibit various forms of bianisotropy, their effects are most often negligible [74]. Hence, the use of artificially engineered materials becomes necessary. In this section, we initially focus on general guidelines for synthesizing bianisotropic materials, considering their time and space-reversal symmetries. Subsequently, we provide an overview of existing and potential new material realizations of time-modulated media based on these principles. Some parts of this section are based on the results presented in [75].

4.1. Time-reversal symmetry

Microscopic Maxwell's equations obey time-reversal symmetry. Indeed, it is easy to check that under the swap $t \to -t$, $\mathbf{E}(t) \to \mathbf{E}(-t)$, and $\mathbf{B}(t) \to -\mathbf{B}(-t)$, the form of the equations remains the same [75] (for brevity, we omit here external sources). In the frequency domain, it translates to the fact that for each electromagnetic process described by fields $\mathbf{E}(\omega)$ and $\mathbf{B}(\omega)$ there is a reverse process with fields $\mathbf{E}^*(\omega)$ and $-\mathbf{B}^*(\omega)$ propagating in the opposite direction. On the contrary, time-reversal symmetry of macroscopic Maxwell's equations can be *locally* broken due to material dissipation or the presence of an external bias field influencing the material response. Time-reversal symmetry holds for all known electromagnetic phenomena when applied in the "global" sense to all the thermodynamic effects (that is, when loss is reversed into corresponding gain) and to all the external bias sources [76]. For example, conventional wisdom suggests that when light is transmitted through a lossy medium, resulting in its attenuation, and then sent in

Optical Materials EXPRESS

the opposite direction, it will not return to its original intensity. Conversely, in the case of light passing through a magneto-optical medium under the influence of a static external magnetic field, the processes of original and reversed wave propagation will not differ if the external field is reversed for the opposite propagation scenario.

Depending on how they transform under time-reversal operation, it is convenient to classify the material tensors into two groups, namely "time-even" (TE) and "time-odd" (TO). Let us rewrite constitutive relations (1) in a general bianisotropic medium in the following form assuming that the material tensors are functions of an arbitrary bias vector $\mathbf{Q}$ that defines some external physical quantity (e.g., magnetic field, electric current, velocity, etc.) that affects the response of the material to light:

$$\begin{aligned}\mathbf{D}(\omega) &= \bar{\bar{\varepsilon}}(\omega,\mathbf{Q})\cdot\mathbf{E}(\omega) + \bar{\bar{\xi}}(\omega,\mathbf{Q})\cdot\mathbf{H}(\omega),\\ \mathbf{B}(\omega) &= \bar{\bar{\zeta}}(\omega,\mathbf{Q})\cdot\mathbf{E}(\omega) + \bar{\bar{\mu}}(\omega,\mathbf{Q})\cdot\mathbf{H}(\omega).\end{aligned} \tag{11}$$

We can split each material tensor into two parts that constitute linear (higher-order material parameter dependencies are typically much weaker in strength) dependence on time-even vector $\mathbf{Q}_{\mathrm{TE}}$ and time-odd vector $\mathbf{Q}_{\mathrm{TO}}$. In the example of the bianisotropic tensor, this separation would correspond to $\bar{\bar{\xi}}_{\mathrm{TE}}(\omega,\mathbf{Q}_{\mathrm{TE}}) = \bar{\bar{\xi}}_1(\omega) + \bar{\bar{\xi}}_2(\omega)\mathbf{Q}_{\mathrm{TE}}$ and $\bar{\bar{\xi}}_{\mathrm{TO}}(\omega,\mathbf{Q}_{\mathrm{TO}}) = \bar{\bar{\xi}}_3\mathbf{Q}_{\mathrm{TO}}$, respectively, where $\bar{\bar{\xi}}_1$, $\bar{\bar{\xi}}_2$, and $\bar{\bar{\xi}}_3$ are arbitrary tensors. The absence of dependence on any external vector is modeled by assuming $\mathbf{Q}_{\mathrm{TE}} = \mathbf{Q}_{\mathrm{TO}} = 0$. Applying the *global* time reversal to constitutive relations °class1, we obtain the following relation between the bianisotropic tensors in the time-reversed and original materials [75]:

$$\begin{aligned}&\bar{\bar{\xi}}_1'(\omega) = -\bar{\bar{\xi}}_1^*(\omega),\\ &\bar{\bar{\xi}}_2'(\omega,\mathbf{Q}_{\mathrm{TE}}) = -\bar{\bar{\xi}}_2^*(\omega,\mathbf{Q}_{\mathrm{TE}}),\\ &\bar{\bar{\xi}}_3'(\omega,\mathbf{Q}_{\mathrm{TO}}) = \bar{\bar{\xi}}_3^*(\omega,\mathbf{Q}_{\mathrm{TO}}),\\ &\bar{\bar{\zeta}}_1'(\omega) = -\bar{\bar{\zeta}}_1^*(\omega),\\ &\bar{\bar{\zeta}}_2'(\omega,\mathbf{Q}_{\mathrm{TE}}) = -\bar{\bar{\zeta}}_2^*(\omega,\mathbf{Q}_{\mathrm{TE}}),\\ &\bar{\bar{\zeta}}_3'(\omega,\mathbf{Q}_{\mathrm{TO}}) = \bar{\bar{\zeta}}_3^*(\omega,\mathbf{Q}_{\mathrm{TO}}),\end{aligned} \tag{12}$$

where primes denote time-reversed tensors and the negative signs appear due to the fact that $\mathbf{Q}_{\mathrm{TO}}$ flips its sign under time reversal. Tensors transformed under time reversal as $\bar{\bar{\xi}}_1$, $\bar{\bar{\xi}}_2$, $\bar{\bar{\zeta}}_1$, and $\bar{\bar{\zeta}}_2$ are referred to as time-odd, while tensors like $\bar{\bar{\xi}}_3$ and $\bar{\bar{\zeta}}_3$ are time-even.

Relations (12) are fairly general and apply to all linear time-invariant materials, both passive and active material systems. Assuming passivity, we can use the Onsager-Casimir relations to decompose the bianisotropic tensors and rewrite (12) as

$$\bar{\bar{\kappa}}'(\omega,\mathbf{Q}_{\mathrm{TE}}) = \bar{\bar{\kappa}}^*(\omega,\mathbf{Q}_{\mathrm{TE}}), \qquad \bar{\bar{\chi}}'(\omega,\mathbf{Q}_{\mathrm{TO}}) = \bar{\bar{\chi}}^*(\omega,\mathbf{Q}_{\mathrm{TO}}). \tag{13}$$

Both reciprocal coupling (chirality and omega coupling) $\bar{\bar{\kappa}}$ and Tellegen $\bar{\bar{\chi}}$ tensors are time-odd. The non-zero Tellegen tensor requires the presence of a time-odd bias $\mathbf{Q}_{\mathrm{TO}}$ in a *passive* material, while the chirality tensor can appear in materials biased by a time-even field $\mathbf{Q}_{\mathrm{TE}}$ (e.g., external electric field) or materials without any bias (the special case when $\mathbf{Q}_{\mathrm{TE}} = 0$).

4.2. Space-inversion symmetry

Next, we delve into how material tensors respond to spatial inversion, focusing on their properties concerning parity. As previously mentioned, the presence of a nonreciprocal Tellegen effect in a material hinges on its reaction to an external parameter characterized by time-odd symmetry, denoted as $\mathbf{Q}_{\mathrm{TO}}$. Additionally, for a material to exhibit a particular type of bianisotropic response, it is crucial to examine the spatial symmetry characteristics of its constituents.

Optical Materials EXPRESS

Under spatial inversion (point reflection), all three spatial projections of a polar (true) vector such as the electric field **E** flip their signs so that the resultant vector is **E** [61, p. 268]. Some vectors, including the magnetic field **B** and axial rotation $\_\sigma$, are called axial (pseudovectors) because they transform under spatial inversion similarly to the polar vectors but with an additional sign flip [75]. Likewise, one can differentiate true and pseudotensors. A tensor is classified as a true tensor if it, when dot-multiplied with a true (pseudo) vector, yields a true (pseudo) vector. Conversely, a tensor is deemed a pseudotensor if its dot product with a pseudo (true) vector results in a true (pseudo) vector. Considering the parity symmetry characteristics of electromagnetic field quantities, we revisit the constitutive relations (11). From this analysis, it follows that $\bar{\bar{\kappa}}$ and $\bar{\bar{\chi}}$ are pseudotensors. For practical purposes, it is useful to decompose these pseudotensors into their symmetric and antisymmetric components. Thus, we express $\bar{\bar{\kappa}}(\omega, \mathbf{Q}_{\mathrm{TE}})$ and $\bar{\bar{\chi}}(\omega, \mathbf{Q}_{\mathrm{TO}})$ as the sum of its symmetric and antisymmetric parts

$$\begin{aligned} \bar{\bar{\kappa}}(\omega, \mathbf{Q}_{\mathrm{TE}}) &= \bar{\bar{\kappa}}_{\mathrm{s}}(\omega, \mathbf{Q}_{\mathrm{TE}}) + \Omega(\omega, |Q_{\mathrm{TE}}|)\mathbf{Q}_{\mathrm{TE}} \times \bar{\bar{I}}, \\ \bar{\bar{\chi}}(\omega, \mathbf{Q}_{\mathrm{TO}}) &= \bar{\bar{\chi}}_{\mathrm{s}}(\omega, \mathbf{Q}_{\mathrm{TO}}) + V(\omega, |Q_{\mathrm{TO}}|)\mathbf{Q}_{\mathrm{TO}} \times \bar{\bar{I}}. \end{aligned} \tag{14}$$

Both symmetric and antisymmetric tensor components in (14) are pseudotensors. Importantly, depending on the spatial inversion symmetry of the bias field $\mathbf{Q}_{\mathrm{TE/TO}}$ (being a true or a pseudovector), there are two distinct scenarios for achieving each of the material tensors in (14). For example, material pseudotensor $\bar{\bar{\kappa}}_{\mathrm{s}}(\omega, \mathbf{Q}_{\mathrm{TE}})$ can be generated in a medium with inversion symmetry if it is biased by a time-even pseudovector $\mathbf{Q}_{\mathrm{TE}}$. An alternative route is to create a medium without any bias field ($\mathbf{Q}_{\mathrm{TE}} = 0$) but with inherently broken inversion symmetry. Both routes would result in a tensor $\bar{\bar{\kappa}}_{\mathrm{s}}$ of the same type.

4.3. Possible material platforms

It is essential to highlight that satisfying the specified material symmetries is a necessary condition for achieving bianisotropic phenomena in materials; however, it is not a sufficient condition on its own. In some cases under consideration, additional symmetry breaking may be necessary, but delving into this aspect deviates from the primary focus of this study. Moreover, the strength of the synthesized bianisotropic coupling could be vanishing if the bias field does not effectively "couple" to the material response to light. Furthermore, for the sake of simplicity, our discussion on potential material platforms will primarily concentrate on the development of materials exhibiting a uniaxial bianisotropic response in the plane. We note that the conclusions drawn in this section are applicable only to material systems with linear, time-invariant, and passive response.

Chirality-type bianisotropy's manifestations are fundamentally governed by time- and space-inversion symmetries, leading to two primary methods of realization. Figure 7(a) (left panel) illustrates a typical configuration of a symmetric chirality tensor $\bar{\bar{\kappa}}_{\mathrm{s}}(\omega, \mathbf{Q}_{\mathrm{TE}})$ through a uniaxial blend of metallic or dielectric helices, reminiscent of the Pasteur medium. This approach does not necessitate an external bias ($Q_{\mathrm{TE}} = 0$); however, the medium components must exhibit shapes lacking space-inversion symmetry. Alternatively, a less conventional method can be employed, where the meta-atoms themselves are not intrinsically chiral (i.e., they maintain inversion symmetry), but material chirality is induced through a complex chiral-type external bias. This concept is depicted in Fig. 7(a) (right panel). The requisite chiral bias should be a time-even pseudovector, possibly generated by concurrent linear velocity **v** and angular velocity σ, as illustrated. This approach aligns with predictions in earlier literature (refer to Section 1.9.5, Fig. 1.21 in [74]). It is crucial to note that while two general pathways to achieve chiral bianisotropic response are outlined, their potential realizations are virtually limitless. For instance, Fig. 7 includes examples of external biases, $\mathbf{Q}_{\mathrm{TE}}$ or $\mathbf{Q}_{\mathrm{TO}}$, that could facilitate each type of bianisotropy. Specifically, as depicted in Fig. 7(a) (right panel), employing a bias in the form

Optical Materials EXPRESS

of $\mathbf{Q}_{\mathrm{TE}} = \mathbf{B} \cdot \mathbf{v}$ is feasible. This corresponds to utilizing a gyrotropic medium, magnetized by external field $\mathbf{B}$, in linear motion at speed $\mathbf{v}$, as detailed in Section 7.4c of Kong's book and Section 5 of Dmitriev's work [26,77].

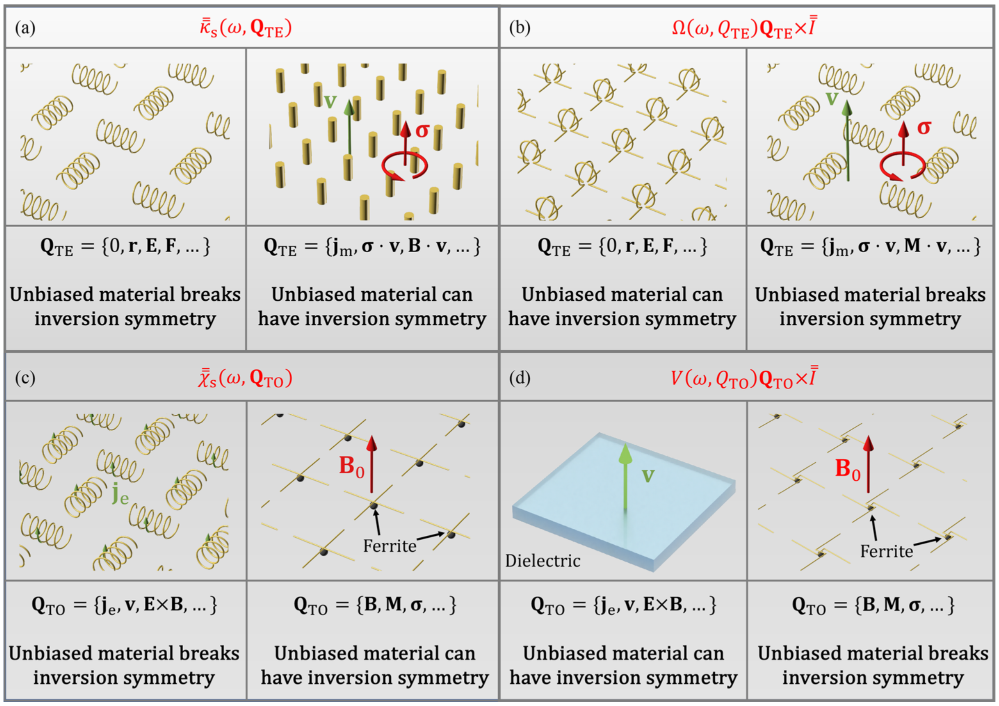

Fig. 7. Conceptual material platforms for realizing different bianisotropic responses. Two characteristic examples are shown for each type of bianisotropy. (a) and (b) Implementation of symmetric and antisymmetric chirality tensors, respectively. Inside the figure brackets different possible biases are listed. (c) and (d) Implementation of symmetric and antisymmetric Tellegen tensors, respectively. Vectors $\mathbf{j}_{\mathrm{e}}$, $\mathbf{j}_{\mathrm{m}}$, $\mathbf{v}$, σ, and $\mathbf{r}$ stand for electric current, effective magnetic current, linear velocity, axial rotation velocity, and radius-vector, respectively. Reprinted with permission from [75].

While various geometrical configurations have been proposed for creating time-invariant bianisotropic media, not all are practical for achieving rapid, single or periodic temporal shifts in bianisotropic coupling. Given that these temporal jumps need to occur within extremely brief time frames, ranging from microseconds to nanoseconds, implementations allowing for electronic modulation of material properties are deemed most suitable. For instance, a feasible unit cell design for a material exhibiting chirality-type temporal boundaries is illustrated in Fig. 8(a). This design incorporates two standard metallic helices [27, p. 128]. One helix is left-handed and time-invariant, while the handedness of the other oscillates between right and left. This alternation is achieved through a straightforward circuit comprising four switches, as shown in the inset. Utilizing this elementary electronic switch setup enables rapid transition between chiral states (when both helices share the same handedness) and achiral, racemic states (where chirality is neutralized due to an equal mix of right- and left-handed helices).

Response modelled by an antisymmetric tensor $\Omega(\omega, |Q_{\mathrm{TE}}|)\mathbf{Q}_{\mathrm{TE}} \times \bar{\bar{I}}$ can be generated in an achiral omega medium, where $\mathbf{Q}_{\mathrm{TE}} = \mathbf{r}$, without necessitating an external field ($\mathbf{r}$ is the radius-vector). This configuration is exemplified in Fig. 7(b) (left panel) [30]. An alternative approach involves designing a material geometry with disrupted inversion symmetry, as depicted

Optical Materials EXPRESS

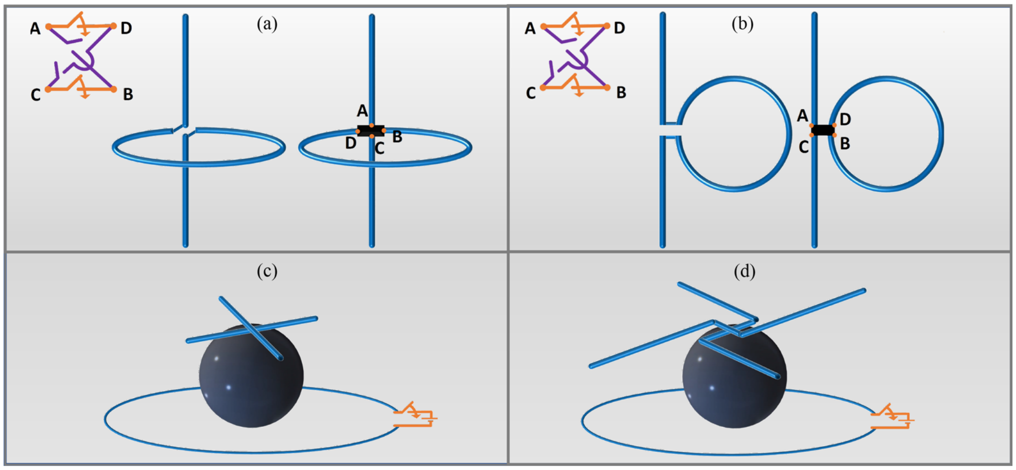

Fig. 8. Conceptual unit cells of materials capable of exhibiting temporal jumps of bianisotropic coupling. (a–b) Chiral and omega unit cells incorporating circuitry of four switches. (c–d) Unit cells capable of tunable Tellegen and artificial velocity couplings. When the switch is on, a DC electric current is flowing through the metallic loop, generating an axial magnetic field that biases the ferrite sphere of the particle. Figures adapted from [64].

in the right panel of the same figure. However, in this case, to maintain the desired properties, it becomes necessary to counterbalance the inherent chirality with an added external time-even pseudovector field (so that in this case $\Omega(\omega, |Q_{\mathrm{TE}}|)\mathbf{Q}_{\mathrm{TE}} \times \bar{\bar{I}}$ in (14) remains a pseudotensor). This method appears considerably more complex compared to the former. A conceptual model for a metamaterial unit cell capable of achieving temporal jumps in omega-type bianisotropy is illustrated in Fig. 8(b). In this design, akin to the previously mentioned chiral scenario, one metallic particle maintains a constant omega-shaped structure. Conversely, the other particle can toggle between this standard omega shape and an altered "twisted" omega configuration [78]. When the latter state is active, it results in the neutralization of the overall omega coupling.

We now turn our attention to materials that facilitate nonreciprocal Tellegen and artificial velocity effects. Intriguingly, these materials exhibit nonreciprocal properties even without temporal modulation. It is important to note that such effects cannot be solely attributed to spatial inhomogeneities; an external bias is essential, as seen in Fig. 7. This requirement has led to a relatively sparse body of research on these material types. For instance, response corresponding to the symmetric Tellegen tensor $\bar{\bar{\chi}}_{\mathrm{s}}(\omega, \mathbf{Q}_{\mathrm{TO}})$ can be realized in a medium with broken inversion symmetry, biased by an external time-odd true vector field such as electric current $\mathbf{j}_{\mathrm{e}}$, as depicted in Fig. 7(c) (left panel). A practical example of this would be an electron plasma with incorporated helical meta-atoms, biased by a DC electric current. Another established approach employs achiral meta-atoms with ferrite components, biased by a pseudovector external magnetic field $\mathbf{B}_0$ [79,80], as shown in Fig. 7(c) (right panel). Here, the yellow wires atop the ferrite spheres represent metallic strips. While this design is confined to the microwave frequency range, recent proposals have introduced a Tellegen optical metamaterial based on spontaneous magnetization, eliminating the need for an external magnetic field [81,82]. It is also noteworthy that magnetoelectric properties akin to the Tellegen effect naturally occur in materials such as topological insulators and multi-ferroic media, but these are typically very weak effects at high frequencies [83,84]. For temporal modulation of the Tellegen response, a simple meta-atom design is proposed in Fig. 8(c). In this setup, an external magnetic field is applied to the ferrite

Optical Materials EXPRESS

sphere by driving a DC current through a metallic loop. An electronic switch adjusts the bias field's amplitude, thereby controlling the Tellegen coupling strength.

Effects due to a non-zero antisymmetric tensor $V(\omega, |Q_{\mathrm{TO}}|)\mathbf{Q}_{\mathrm{TO}} \times \bar{\bar{I}}$ (velocity or artificial velocity) can be achieved in an isotropic dielectric medium moving with linear speed $\mathbf{v}$, as outlined in [26, Section 7.4a] and [85]. An alternative realization involves a medium with broken inversion symmetry, biased by an external pseudovector like the magnetic flux density $\mathbf{B}_0$, as depicted in Fig. 7(d). Notably, intriguing approaches diverging from the first include using dielectric scatterers in rotational motion with angular speed $\mathbf{v} = \Omega \times \mathbf{r}$ [86–88], synthesizing motion [89], and leveraging materials biased by orthogonal static electric and magnetic fields, leading to V being proportional to $\mathbf{E} \times \mathbf{B}$ [90–92]. Structures utilizing the artificial velocity parameter have been proposed for both optical and microwave regimes [79,93–97] and have seen experimentally confirmed in [92,98,99]. Additionally, a similar symmetry effect for phonons was recently considered [100]. Time modulation of the artificial velocity tensor, akin to the Tellegen response, can be controlled using a switch to modulate the DC current magnetizing meta-atoms, as shown in Fig. 8(d). An alternative mechanism for dynamic artificial velocity involves a gyrator circuit, as proposed in [99]. This method operates in a deeply sub-wavelength regime, but so far has been realized only in the transmission-line environment.

The principles of space and time inversion symmetries offer a fundamental classification of all possible linear effects in matter. This approach not only simplifies understanding but also draws parallels between various effects that share a common physical origin. Using these principles helps to identify realizations that are most amenable for creation of dynamic bianisotropic media.

4.4. Bianisotropic metamaterials based on active systems

In the previous section, we discussed the creation of various bianisotropic materials using linear, time-invariant, passive systems. Upon removing the constraint of passivity, the limitations (13) imposed by time-reversal symmetry no longer apply, rendering the symmetry considerations outlined in Fig. 7 invalid. Specifically, active systems do not necessarily adhere to the Onsager-Casimir relations, and time-reversal symmetry only provides the general relations detailed in (12). In particular, these relations indicate that both the symmetric and antisymmetric components of the $\bar{\bar{\xi}}$ and $\bar{\bar{\zeta}}$ tensors can be generated using a time-even bias field, such as an electric field $\mathbf{E}$. Practically speaking, time-even biases are often preferable. For instance, establishing and maintaining a static voltage bias is more energy-efficient than generating a static magnetic field bias, which usually requires an electric current and leads to Ohmic dissipation. Pioneering studies [102–104] demonstrated that Faraday rotation, a gyrotropic nonreciprocal effect, can be achieved in systems that incorporate common-source field-effect transistors with a time-even (static voltage) bias. In these systems, active transistors can function as isolators, matched electrical components that restrict wave propagation to one direction. A recent advancement in this field was the adaptation of this concept for designing nonreciprocal bianisotropic metasurfaces, as reported in [101]. Figures 9(a) and (b) show two bianisotropic time-invariant metasurface designs, each comprising three layers with arrows indicating the positions and current transmission directions of lumped isolators. In these designs, a static voltage serves as the bias. These meta-atoms resemble those in earlier passive structures (refer to Figs. 7(c) and (d) (right panels)) and can be classified as Tellegen and artificial velocity types, respectively. The use of voltage bias in the meta-atom suggests that these metamaterials could be modulated at electronic speeds, positioning them as potential candidates for implementing temporal variations in nonreciprocal bianisotropic media. In contrast, realizations shown in Figs. 7(c) and (d) (right panels) rely on a static magnetic field produced by an external electromagnet, which exhibits relatively low modulation speeds owing to the inductance of its coils.

Optical Materials EXPRESS

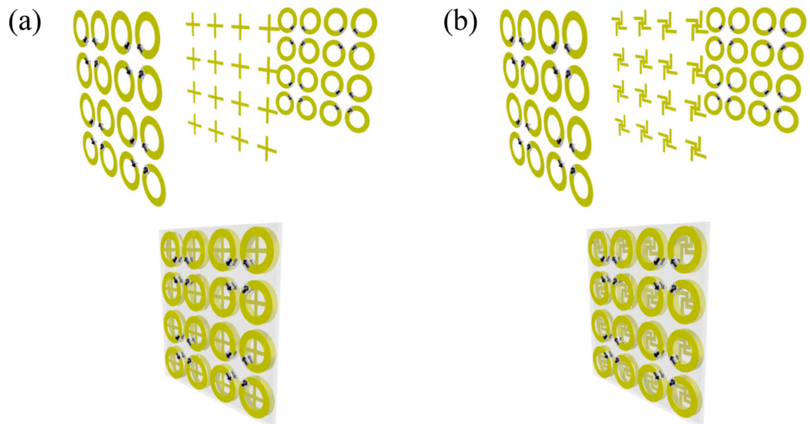

Fig. 9. Schematics of two nonreciprocal bianisotropic active metasurfaces possessing the Tellegen (a) and artificial-velocity (b) response. The yellow color denotes metallization and the arrows depict electronic isolators that could be realized with common-source field-effect transistors. Figures adapted with permission from [101].

4.5. Bianisotropic metamaterials based on space-time-varying systems

Space-time varying structures can be used for the realization of bianisotropic effects because the required bias vectors $\mathbf{Q}_{\rm TE}$ or $\mathbf{Q}_{\rm TO}$ (see Fig. 7) can be defined by externally imposed space-time variations of the structure parameters. Let us first discuss such realizations of bianisotropic effects with antisymmetric nonreciprocal coupling characterized by the artificial velocity parameter V. We see from Fig. 7(d) that vectors defining the biasing mechanism must be true vectors, for instance, linear velocity. This is actually expected from the simple fact that the material relations for fields in a homogeneous unbounded moving medium seen in a reference frame at rest are the same as the material relations of a stationary bianisotropic medium of this class, e.g. [26,27]. To create the corresponding effects, it is not necessary to physically move the material sample. Instead, it is possible to use space-time modulation of its material parameters in the form of a wave traveling along a certain direction. Such modulations were introduced probably by Cullen, Tien, and Suhl (1958) [105,106]. In contrast to even earlier developed traveling-wave tubes where electromagnetic waves interacted with a beam of moving electrons, in parametric traveling-wave amplifiers electromagnetic waves interact with space-time modulations of a stationary transmission line. The strongest effects are achieved under the condition of equality of the phase velocity of the electromagnetic waves and the modulation velocity (the so-called luminal regime). Equivalence of space-time modulated media (wave-type modulation) and bianisotropic media exhibiting artificial velocity coupling was discussed in [107–109]. As was shown in these papers, the equivalence requires that both permittivity and permeability are modulated in space and time (see illustration in Fig. 10(a)). Importantly, the long-wavelength regime is assumed, to ensure that inevitable frequency conversions in time-varying media can be neglected, as the frequency is conserved in stationary linear bianisotropic materials. In these settings, the phase velocity vector $\mathbf{c}_{\rm g}$ of the modulation wave defines the symmetry-breaking direction in space (the required biasing true vector $\mathbf{Q}_{\rm TO}$).

It is also possible to define a time-even bias with space-time modulations. Indeed, in recent work [110], the space-time modulation mimicked both the linear velocity of the medium and its rotational motion around the same axis via modulating the anisotropy axis of the medium. The geometry of the proposed structure is shown in Fig. 10(b). The authors of that work refer to such material as chiral in the sense of circular-polarization-selective amplification. Importantly,

Optical Materials EXPRESS

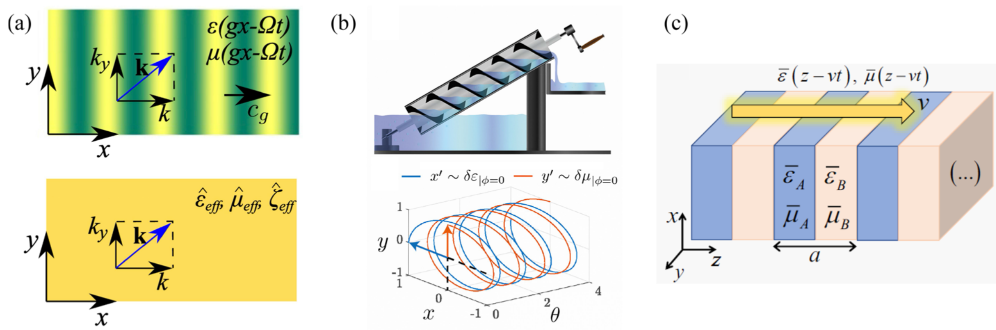

Fig. 10. (a) Equivalence of wave propagation in a medium with space–time traveling-wave–modulated permittivity and permeability (top) with that in a bianisotropic medium with artificial-velocity coupling $\hat{\zeta}_{\rm eff}$ (bottom). Here, g and Ω are the spatial and temporal frequencies of the space-time modulation, $c_{\rm g} = \Omega/g$, and k and k_y are the wave vectors along the modulation direction and orthogonal to it, respectively. Figure adapted with permission from [107]. (b) Top: A mechanical analogy of the chiral space-time medium. Archimedes screw carries fluids from a lower to a higher ground. Bottom: An electromagnetic chiral space-time medium whose permittivity and permeability tensors are modulated such that the principal axes $\delta\varepsilon$ and $\delta\mu$ of their modulation describe two helices (adapted from [110]). (c) Schematic of an anisotropic space-time crystal formed by two magneto-electric layers. The arrow indicates how the material parameters vary in time (adapted with permission from [111]).

without space-time modulations, the background material has inversion symmetry. The effective chirality can be induced due to the space-time modulations, which are described by a time-even pseudovector bias $\mathbf{Q}_{\rm TE}$ (linear and angular velocities combined). Therefore, this configuration in the long-wavelength limit appears similar to the material response shown in the right panel of Fig. 7(a).

Recently, a novel approach for realizing a nonreciprocal Tellegen medium using space-time-varying systems was proposed in [111]. This approach involves a space-time crystal, featuring appropriate glide-rotation symmetry and composed of magneto-electric material (see Fig. 10(c)) that can be homogenized in the long-wavelength limit to yield a Tellegen-and/or artificial-velocity-type material. While the bias field here is represented by space-time modulation emulating only linear velocity (true time-odd bias vector $\mathbf{Q}_{\rm TO}$), the unbiased material itself breaks inversion symmetry due to its glide-rotational geometry (each unit cell consists of two mutually shifted anisotropic slabs). Therefore, inside such a material, the Tellegen response in the long-wavelength limit is similar to that shown in the left panel of Fig. 7(c).

The space-time-modulated schemes discussed above offer viable material platforms for practically implementing temporal bianisotropy jumps and other time-varying bianisotropic systems. Interestingly, realizations of time-varying bianisotropic media based on space-time modulations require time modulating (switching) of an already modulated structure. Perhaps this approach can be called “metamodulation”. Nevertheless, these schemes present a challenge due to the dual modulation requirement of both permittivity and permeability, which necessitates further investigations on material realizations.

5. Discussion and research outlook

In this overview we have highlighted that anisotropic and especially bianisotropic time-varying media exhibit significant potential for non-trivial temporal scattering wave phenomena. Notably, functionalities such as polarization manipulation and wave steering can be effectively carried

Optical Materials EXPRESS

out at anisotropic temporal interfaces. Moreover, the revealed asymmetric frequency and energy transformations at bianisotropic temporal interfaces shed light on their capability for unconventional wave control in various applications. We have reviewed guidelines for synthesizing bianisotropic metamaterials and presented some possibilities for their time modulation. The choice of a suitable material platform for exploration of time-varying complex media depends on the possibilities for external control of the coupling strength. However, some of the possible platforms for realization of bianisotropic effects need more considerations of possible mechanisms for tunability or temporal modulation of bianisotropic coupling. In this respect, realizations based on active systems and on space-time modulations appear to be most promising, and they are of special interest.

The time-domain material relations of bianisotropic media in (8) assume that all oscillations are at the frequencies well below all resonances of meta-atoms, and that all spatial dispersion effects are weak, only up to the first order. Further investigations are needed to develop better understanding of strongly dispersive, resonant time-varying bianisotropic materials. This research direction holds significant importance as the exploitation of resonances enables the realization of strong effects in field-matter interactions.

We have seen that so far only a few initial studies of field effects in time-varying bianisotropic media have been conducted, basically limited to single time jumps of various coupling coefficients in isotropic or uniaxial bianisotropic materials. Even these initial works have revealed novel physical effects, showing possibilities to create direction-dependent and polarization-dependent temporal scattering. We see significant potential in developing bianisotropic media that are periodically modulated in time, bianisotropic photonic time crystals. Wave amplification in conventional photonic time crystals is limited by reciprocity of the modulated material and its symmetries. In this respect, even anisotropic photonic time crystals (without magnetoelectric coupling) are of significant interest. For instance, as explained above, a temporal interface between free space and magnetoplasma provides a possibility to manipulate polarization of electromagnetic waves. Thus, one can naturally think about anisotropic temporal slabs (creation and destruction of plasma in the presence of a static magnetic field [112] or time modulation of the external bias field inside a plasma volume) and eventually about obtaining anisotropic photonic time crystals. More general bianisotropic photonic time crystals present a promising avenue for achieving even more complete control over nonreciprocal and polarization-dependent wave amplification.

Furthermore, it is necessary to develop understanding of bianisotropic spatiotemporal interfaces and other bianisotropic structures that are nonuniform both in time and space. Of particular interest are time-modulated bianisotropic metasurfaces that hold the potential of controlling conversions of not only wavevectors and polarizations but also the frequencies of reflected and transmitted waves.

Funding. Horizon 2020 Framework Programme (PULSE); Research Council of Finland (330260, 356797, Flagship Programme (PREIN Aalto University Project No. 346529)).

Disclosures. The authors declare no conflicts of interest.

Data availability. There are no data beyond those presented in the text.

References

1. N. Engheta and R. W. Ziolkowski, *Metamaterials: Physics and Engineering Explorations* (IEEE-Wiley, 2006).
2. F. Capolino, editor, *Metamaterials Handbook: Theory and Phenomena of Metamaterials* (CRC Press, 2009).
3. K. Achouri and C. Caloz, *Electromagnetic Metasurfaces: Theory and Applications* (Wiley – IEEE Press, 2021).
4. F. Yang and Y. Rahmat-Samii, *Surface Electromagnetics, with Applications in Antenna, Microwave, and Optical Engineering* (Cambridge University Press, 2019).
5. C. Caloz and Z.-L. Deck-Léger, "Spacetime metamaterials—part I: General concepts," IEEE Trans. Antennas Propag. **68**(3), 1569–1582 (2020).
6. C. Caloz and Z.-L. Deck-Léger, "Spacetime metamaterials—part II: Theory and applications," IEEE Trans. Antennas Propag. **68**(3), 1583–1598 (2020).

Optical Materials EXPRESS

7. N. Engheta, "Metamaterials with high degrees of freedom: space, time, and more," Nanophotonics **10**(1), 639–642 (2020).
8. E. Galiffi, R. Tirole, and S. Yin, "Photonics of time-varying media," Adv. Photonics **4**(01), 014002 (2022).
9. V. Pacheco-Pe na and N. Engheta, "Merging effective medium concepts of spatial and temporal media: Opening new avenues for manipulating wave-matter interaction in 4D," IEEE Antennas Propag. Mag. **65**(4), 39–49 (2023).
10. G. Ptitcyn, M. S. Mirmoosa, A. Sotoodehfar, *et al.*, "A tutorial on the basics of time-varying electromagnetic systems and circuits: Historic overview and basic concepts of time-modulation," IEEE Antennas Propag. Mag. **65**(4), 10–20 (2023).
11. S. Yin, E. Galiffi, G. Xu, *et al.*, "Scattering at temporal interfaces: An overview from an antennas and propagation engineering perspective," IEEE Antennas Propag. Mag. **65**(4), 21–28 (2023).
12. N. Engheta, "Four-dimensional optics using time-varying metamaterials," Science **379**(6638), 1190–1191 (2023).
13. Z. Hayran and F. Monticone, "Using time-varying systems to challenge fundamental limitations in electromagnetics: Overview and summary of applications," IEEE Antennas Propag. Mag. **65**(4), 29–38 (2023).
14. F. R. Morgenthaler, "Velocity modulation of electromagnetic waves," IEEE Trans. Microwave Theory Techn. **6**(2), 167–172 (1958).
15. J. Mendonça and P. Shukla, "Time refraction and time reflection: two basic concepts," Phys. Scr. **65**(2), 160–163 (2002).
16. D. Ramaccia, A. Alù, A. Toscano, *et al.*, "Temporal multilayer structures for designing higher-order transfer functions using time-varying metamaterials," Appl. Phys. Lett. **118**(10), 101901 (2021).
17. G. Castaldi, M. Moccia, N. Engheta, *et al.*, "Herpin equivalence in temporal metamaterials," Nanophotonics **11**(20), 4479–4488 (2022).
18. G. Castaldi, C. Rizza, N. Engheta, *et al.*, "Multiple actions of time-resolved short-pulsed metamaterials," Appl. Phys. Lett. **122**(2), 021701 (2023).
19. E. Lustig, O. Segal, and S. Saha, "Photonic time-crystals - fundamental concepts," Opt. Express **31**(6), 9165–9170 (2023).
20. P. A. Sturrock, "Kinematics of growing waves," Phys. Rev. **112**(5), 1488–1503 (1958).
21. D. Holberg and K. Kunz, "Parametric properties of fields in a slab of time-varying permittivity," IEEE Trans. Antennas Propag. **14**(2), 183–194 (1966).
22. J. R. Zurita-Sánchez, P. Halevi, and J. C. Cervantes-González, "Reflection and transmission of a wave incident on a slab with a time-periodic dielectric function $\epsilon(t)$," Phys. Rev. A **79**(5), 053821 (2009).
23. X. Wang, M. S. Mirmoosa, and V. S. Asadchy, "Metasurface-based realization of photonic time crystals," Sci. Adv. **9**(14), eadg7541 (2023).
24. E. Lustig, Y. Sharabi, and M. Segev, "Topological aspects of photonic time crystals," Optica **5**(11), 1390–1395 (2018).
25. S. Yin, E. Galiffi, and A. Alù, "Floquet metamaterials," eLight **2**(1), 8 (2022).
26. J. A. Kong, *Electromagnetic Wave Theory* (EMW Publishing, 2008).
27. A. Serdyukov, I. Semchenko, S. Tretyakov, *et al.*, *Electromagnetics of Bi-anisotropic Materials: Theory and Applications* (Gordon and Breach Science Publishers, 2001).
28. S. Tretyakov, A. Sihvola, A. Sochava, *et al.*, "Magnetoelectric interactions in bi-anisotropic media," J. Electromagn. Waves Appl. **12**(4), 481–497 (1998).
29. V. S. Asadchy and S. A. Tretyakov, "Modular analysis of arbitrary dipolar scatterers," Phys. Rev. Appl. **12**(2), 024059 (2019).
30. V. S. Asadchy, A. Díaz-Rubio, and S. A. Tretyakov, "Bianisotropic metasurfaces: physics and applications," Nanophotonics **7**(6), 1069–1094 (2018).
31. S. B. Glybovski, S. A. Tretyakov, and P. A. Belov, "Metasurfaces: From microwaves to visible," Phys. Rep. **634**, 1–72 (2016). Metasurfaces: From microwaves to visible.
32. H. Li, S. Yin, E. Galiffi, *et al.*, "Temporal parity-time symmetry for extreme energy transformations," Phys. Rev. Lett. **127**(15), 153903 (2021).
33. M. S. Mirmoosa, T. Setälä, and A. Norrman, "Quantum theory of wave scattering from electromagnetic time interfaces," arXiv, arXiv.2312.15178 (2023).
34. E. Galiffi, S. Yin, and A. Alú, "Tapered photonic switching," Nanophotonics **11**(16), 3575–3581 (2022).
35. M. I. Bakunov and A. V. Maslov, "Reflection and transmission of electromagnetic waves at a temporal boundary: comment," Opt. Lett. **39**(20), 6029 (2014).
36. M. I. Bakunov, A. V. Shirokova, M. A. Kurnikov, *et al.*, "Light scattering at a temporal boundary in a lorentz medium," Opt. Lett. **46**(19), 4988–4991 (2021).
37. D. M. Solís, R. Kastner, and N. Engheta, "Time-varying materials in the presence of dispersion: plane-wave propagation in a Lorentzian medium with temporal discontinuity," Photonics Res. **9**(9), 1842–1853 (2021).
38. J. Gratus, R. Seviour, P. Kinsler, *et al.*, "Temporal boundaries in electromagnetic materials," New J. Phys. **23**(8), 083032 (2021).
39. J. Zhang, W. R. Donaldson, and G. P. Agrawal, "Temporal reflection and refraction of optical pulses inside a dispersive medium: an analytic approach," J. Opt. Soc. Am. B **38**(3), 997–1003 (2021).
40. J. Zhang, W. R. Donaldson, and G. P. Agrawal, "Time-domain Fabry–Perot resonators formed inside a dispersive medium," J. Opt. Soc. Am. B **38**(8), 2376–2382 (2021).

Optical Materials EXPRESS

41. M. S. Mirmoosa, T. T. Koutserimpas, and G. A. Ptitcyn, "Dipole polarizability of time-varying particles," New J. Phys. **24**(6), 063004 (2022).
42. A. Sotoodehfar, M. Mirmoosa, and S. Tretyakov, "Waves in linear time-varying dielectric media," in *2022 16th European Conference on Antennas and Propagation (EuCAP)*, (IEEE, 2022), pp. 1–5.
43. E. Yablonovitch, "Spectral broadening in the light transmitted through a rapidly growing plasma," Phys. Rev. Lett. **31**(14), 877–879 (1973).
44. C.-L. Jiang, "Wave propagation and dipole radiation in a suddenly created plasma," IEEE Trans. Antennas Propag. **23**(1), 83–90 (1975).
45. D. K. Kalluri, *Electromagnetics of Time Varying Complex Media: Frequency and Polarization Transformer* (Taylor & Francis, 2010).
46. A. Nishida, N. Yugami, and T. Higashiguchi, "Experimental observation of frequency up-conversion by flash ionization," Appl. Phys. Lett. **101**(16), 1 (2012).
47. A. Shlivinski and Y. Hadad, "Beyond the Bode-Fano bound: Wideband impedance matching for short pulses using temporal switching of transmission-line parameters," Phys. Rev. Lett. **121**(20), 204301 (2018).
48. V. Pacheco-Pe na and N. Engheta, "Antireflection temporal coatings," Optica **7**(4), 323–331 (2020).
49. H. Weinstein, "Linear signal stretching in a time-variant system," IEEE Trans. Circuit Theory **12**(2), 157–164 (1965).
50. J. B. Gunn, "Transformation and reversal of time scale by a time-varying transmission line," Electron. Lett. **2**(7), 247 (1966).
51. V. Bacot, M. Labousse, and A. Eddi, "Time reversal and holography with spacetime transformations," Nat. Phys. **12**(10), 972–977 (2016).
52. H. Moussa, G. Xu, and S. Yin, "Observation of temporal reflection and broadband frequency translation at photonic time interfaces," Nat. Phys. **19**(6), 863–868 (2023).
53. E. Noether, "Invariante variationsprobleme," Nachrichten von der Gesellschaft der Wissenschaften zu Göttingen **1918**, 235–257 (1918).
54. A. Ortega-Gomez, M. Lobet, J. E. Vázquez-Lozano, *et al.*, "Tutorial on the conservation of momentum in photonic time-varying media," Opt. Mater. Express **13**(6), 1598–1608 (2023).
55. D. Kalluri, "Frequency shifting using magnetoplasma medium: flash ionization," IEEE Trans. Plasma Sci. **21**(1), 77–81 (1993).
56. J. Xu, W. Mai, and D. H. Werner, "Complete polarization conversion using anisotropic temporal slabs," Opt. Lett. **46**(6), 1373–1376 (2021).
57. C. Rizza, G. Castaldi, and V. Galdi, "Spin-controlled photonics via temporal anisotropy," Nanophotonics **12**(14), 2891–2904 (2023).
58. V. Pacheco-Pe na and N. Engheta, "Temporal aiming," Light: Sci. Appl. **9**(1), 129 (2020).
59. V. Pacheco-Pe na and N. Engheta, "Temporal equivalent of the brewster angle," Phys. Rev. B **104**(21), 214308 (2021).
60. A. Akbarzadeh, N. Chamanara, and C. Caloz, "Inverse prism based on temporal discontinuity and spatial dispersion," Opt. Lett. **43**(14), 3297–3300 (2018).
61. J. D. Jackson, *Classical Electrodynamics* (American Association of Physics Teachers, 1999).
62. E. U. Condon, "Theories of optical rotatory power," Rev. Mod. Phys. **9**(4), 432–457 (1937).
63. A. H. Sihvola and I. V. Lindell, "Bi-isotropic constitutive relations," Microw. Opt. Technol. Lett. **4**(8), 295–297 (1991).
64. M. S. Mirmoosa, M. H. Mostafa, A. Norrman, *et al.*, "Time interfaces in bianisotropic media," Physical Review Research (to be published).
65. M. H. M. Mostafa, M. S. Mirmoosa, and S. A. Tretyakov, "Spin-dependent phenomena at chiral temporal interfaces," Nanophotonics **12**, 2881–2889 (2023).
66. S. Yin, Y.-T. Wang, and A. Alù, "Temporal optical activity and chiral time-interfaces," Opt. Express **30**(26), 47933–47941 (2022).
67. D. Yang, J. Xu, and D. H. Werner, "A generalized temporal transfer matrix method and its application to modeling electromagnetic waves in time-varying chiral media," Appl. Phys. Lett. **122**(25), 251102 (2023).
68. E. Galiffi, G. Xu, and S. Yin, "Broadband coherent wave control through photonic collisions at time interfaces," Nat. Phys. **19**(11), 1703–1708 (2023).
69. J. R. Reyes-Ayona and P. Halevi, "Observation of genuine wave vector (k or β) gap in a dynamic transmission line and temporal photonic crystals," Appl. Phys. Lett. **107**(7), 074101 (2015).
70. E. Lustig, O. Segal, and S. Saha, "Time-refraction optics with single cycle modulation," Nanophotonics **12**(12), 2221–2230 (2023).
71. R. Tirole, S. Vezzoli, and E. Galiffi, "Double-slit time diffraction at optical frequencies," Nat. Phys. **19**(7), 999–1002 (2023).
72. O. Sakai and K. Tachibana, "Plasmas as metamaterials: a review," Plasma Sources Sci. Technol. **21**(1), 013001 (2012).
73. C. R. Simovski, P. A. Belov, A. V. Atrashchenko, *et al.*, "Wire metamaterials: physics and applications," Adv. Mater. **24**(31), 4229–4248 (2012).
74. L. D. Barron, *Molecular Light Scattering and Optical Activity* (Cambridge University Press, 2009).

75. V. S. Asadchy, M. S. Mirmoosa, and A. Díaz-Rubio, "Tutorial on electromagnetic nonreciprocity and its origins," Proc. IEEE **108**(10), 1684–1727 (2020).
76. R. G. Sachs, *The Physics of Time Reversal* (University of Chicago Press, 1987).
77. V. Dmitriev, "Group theoretical approach to complex and bianisotropic media description," The Eur. Phys. J. - Appl. Phys. **6**(1), 49–55 (1999).
78. V. S. Asadchy, Y. Ra'di, J. Vehmas, *et al.*, "Functional metamirrors using bianisotropic elements," Phys. Rev. Lett. **114**(9), 095503 (2015).
79. S. A. Tretyakov, "Nonreciprocal composite with the material relations of the transparent absorbing boundary," Microw. Opt. Technol. Lett. **19**(5), 365–368 (1998).
80. B. D. Tellegen, "The gyrator, a new electric network element," Philips Res. Rep **3**, 81–101 (1948).
81. S. S. Jazi, I. Faniayeu, R. Cichelero, *et al.*, "Optical Tellegen metamaterial with spontaneous magnetization," (2023).
82. L. Shaposhnikov, M. Mazanov, and D. A. Bobylev, "Emergent axion response in multilayered metamaterials," Phys. Rev. B **108**(11), 115101 (2023).
83. A. D. LaForge, A. Frenzel, and B. C. Pursley, "Optical characterization of Bi_2 Se_3 in a magnetic field: Infrared evidence for magnetoelectric coupling in a topological insulator material," Phys. Rev. B **81**(12), 125120 (2010).
84. A. P. Pyatakov and A. K. Zvezdin, "Magnetoelectric and multiferroic media," Phys.-Usp. **55**(6), 557–581 (2012).
85. Y. Mazor and A. Alù, "Nonreciprocal hyperbolic propagation over moving metasurfaces," Phys. Rev. B **99**(4), 045407 (2019).
86. T. Shiozawa, "Phenomenological and electron-theoretical study of the electrodynamics of rotating systems," Proc. IEEE **61**(12), 1694–1702 (1973).
87. B. Z. Steinberg, A. Shamir, and A. Boag, "Two-dimensional Green's function theory for the electrodynamics of a rotating medium," Phys. Rev. E **74**(1), 016608 (2006).
88. Y. Mazor and B. Z. Steinberg, "Rest frame interference in rotating structures and metamaterials," Phys. Rev. Lett. **123**(24), 243204 (2019).
89. Y. Mazor and A. Alù, "One-way hyperbolic metasurfaces based on synthetic motion," IEEE Trans. Antennas Propag. **68**(3), 1739–1747 (2020).
90. N. B. Baranova, Y. V. Bogdanov, and B. Y. Zel'dovich, "New electro-optical and magneto-optical effects in liquids," Sov. Phys. Usp. **20**(10), 870–877 (1977).
91. H. J. Ross, B. S. Sherborne, and G. E. Stedman, "Selection rules for optical activity and linear birefringence bilinear in electric and magnetic fields," J. Phys. B: At., Mol. Opt. Phys. **22**(3), 459–473 (1989).
92. G. L. J. A. Rikken, C. Strohm, and P. Wyder, "Observation of magnetoelectric directional anisotropy," Phys. Rev. Lett. **89**(13), 133005 (2002).
93. N. B. Baranova and B. Y. Zel'dovich, "Theory of a new linear magnetorefractive effect in liquids," Mol. Phys. **38**(4), 1085–1098 (1979).
94. Y. Mazor and B. Z. Steinberg, "Metaweaves: Sector-way nonreciprocal metasurfaces," Phys. Rev. Lett. **112**(15), 153901 (2014).
95. Y. Park, V. S. Asadchy, and B. Zhao, "Violating kirchhoff's law of thermal radiation in semitransparent structures," ACS Photonics **8**(8), 2417–2424 (2021).
96. M. Mirmoosa, Y. Ra'di, and V. Asadchy, "Polarizabilities of nonreciprocal bianisotropic particles," Phys. Rev. Appl. **1**(3), 034005 (2014).
97. Y. Ra'di, V. S. Asadchy, and S. A. Tretyakov, "One-way transparent sheets," Phys. Rev. B **89**(7), 075109 (2014).
98. G. L. J. A. Rikken and E. Raupach, "Observation of magneto-chiral dichroism," Nature **390**(6659), 493–494 (1997).
99. J. Vehmas, S. Hrabar, and S. Tretyakov, "Transmission lines emulating moving media," New J. Phys. **16**(9), 093065 (2014).
100. M. Hamada and S. Murakami, "Phonon rotoelectric effect," Phys. Rev. B **101**(14), 144306 (2020).
101. Y. Ra'di and A. Grbic, "Magnet-free nonreciprocal bianisotropic metasurfaces," Phys. Rev. B **94**(19), 195432 (2016).
102. T. Kodera, D. L. Sounas, and C. Caloz, "Artificial Faraday rotation using a ring metamaterial structure without static magnetic field," Appl. Phys. Lett. **99**(3), 031114 (2011).
103. Z. Wang, Z. Wang, and J. Wang, "Gyrotropic response in the absence of a bias field," Proc. Natl. Acad. Sci. **109**(33), 13194–13197 (2012).
104. T. Kodera, D. L. Sounas, and C. Caloz, "Magnetless nonreciprocal metamaterial (MNM) technology: Application to microwave components," IEEE Trans. Microwave Theory Tech. **61**(3), 1030–1042 (2013).
105. A. Cullen, "A travelling-wave parametric amplifier," Nature **181**(4605), 332 (1958).
106. P. K. Tien and H. Suhl, "A traveling-wave ferromagnetic amplifier," Proc. IRE **46**(4), 700–706 (1958).
107. P. A. Huidobro, E. Galiffi, and S. Guenneau, "Fresnel drag in space–time-modulated metamaterials," Proc. Natl. Acad. Sci. U. S. A. **116**(50), 24943–24948 (2019).
108. P. Huidobro, M. Silveirinha, E. Galiffi, *et al.*, "Homogenization theory of space-time metamaterials," Phys. Rev. Appl. **16**(1), 014044 (2021).
109. A. Bahrami, Z.-L. Deck-Léger, and C. Caloz, "Electrodynamics of accelerated-modulation space-time metamaterials," Phys. Rev. Appl. **19**(5), 054044 (2023).

Optical Materials EXPRESS

110. E. Galiffi, P. A. Huidobro, and J. B. Pendry, "An Archimedes' screw for light," Nat. Commun. **13**, 1 (2022).
111. F. R. Prudêncio and M. G. Silveirinha, "Synthetic axion response with space-time crystals," Phys. Rev. Appl. **19**(2), 024031 (2023).
112. H. Li, S. Yin, and A. Alù, "Nonreciprocity and Faraday rotation at time interfaces," Phys. Rev. Lett. **128**(17), 173901 (2022).